

Optimal Team Time Trial Strategy in Road Cycling

Optimisation of Changing Strategy using a Mathematical Performance model

M. W. B. Overtoom



Optimal Team Time Trial Strategy in Road Cycling

Optimisation of Changing Strategy using a
Mathematical Performance model

by

M. W. B. Overtoom

to obtain the degree of Master of Science
at the Delft University of Technology,
to be defended publicly on Tuesday January 1, 2013 at 10:00 AM.

Student number:	4178777
Project duration:	March 1, 2012 – January 1, 2013
Thesis committee:	Dr. ir. A. L. Schwab, TU Delft, supervisor
	Dr. D. J. J. Bregman, TU Delft, supervisor
	Dr. A. Sciacchitano, TU Delft
	MSc. T. Van Erp, Team Sunweb

This thesis is confidential and cannot be made public until October 31, 2020.

An electronic version of this thesis is available at <http://repository.tudelft.nl/>.

Abstract

During team time trials in road cycling changing schemes are used to spread the workload over the cyclists in the team. Models that provide predictions of race performance already exist for individual time trials. It is proposed that with a performance model for team time trials, the performance of different strategies can be compared and optimised.

In literature combinations of mechanical resistance models and physiological models are used to determine the performance of individual time trials. The aerodynamic interaction between cyclists is very important to the effectiveness of a strategy. Coefficients of drag reduction between cyclists in a team time trial are presented in several studies, however most studies use groups of only four cyclists, which is not useful for a team time trial with eight cyclists. Only two studies report data for groups up to eight cyclists. These two models show different behaviour and are both used to assess the performance of strategies. Also two physiological models were used.

In the model provided in this study the resistances are calculated from the kinematics resulting from the evaluated strategy. The mechanical resistance model, including the aerodynamic interaction model calculates the power required to perform the strategy. The physiological model calculates the physiology during the race, which determines if the cyclists are able to sustain the prescribed strategy.

Genetic algorithm optimisation is used to optimise the strategy parameters, such as initial position and times spend in first position. The velocity is optimised for each evaluated strategy configuration. A convergence test was performed to determine the parameters for the genetic algorithm, which are used in the optimisation of strategy.

Using the standard strategy, where cyclists only change from first to last position, different orders are compared. From this study it was determined that the mean velocity over a 30 km team time trial could be raised by a maximum of 0.228 m/s by improving the order, depending on the model configuration. It was found that the best performing orders were those where the mean performance difference of following cyclists was lowest.

Two different strategies have been assessed where cyclists still always change from first, but not necessarily last position have been assessed on their performance. With those more complex strategies the mean velocity could be increased with 0.358 m/s over a 30 km team time trial.

The model still lacks validity, but gives a relevant insight in the performance of different team time trial strategies. The validity can either be improved by using track test to validate the drag reduction coefficients or by using power data from a team time trial to show that the model predicts realistic physiology. Of those two methods the last is preferred.

Preface

This document contains the research results for the final research (thesis) for the Master Mechanical Engineering, Track Biomechanical Design and specialisation Sports Engineering, part of the faculty of Mechanical, Maritime and Materials Engineering, Delft Technical University. The project has been performed in collaboration with Cycling Team, Team Sunweb

This reports will present a mathematical model to estimate the performance of strategies in a team time trial in road cycling, as well as the analysis of several suggested strategies for a team time trial.

I would like to thank my university committee: Dr. ir. A. L. Schwab, Dr. D. J. J. Bregman, Dr. A. Sciacchitano and company mentor Msc. T Van Erp for their academic support, my friends family and study mates for their daily support during the period of this research.

*M. W. B. Overtoom
Delft, October 2018*

Contents

Abstract	iii
1 Introduction	1
1.1 List of symbols	3
2 Modelling of the team time trial performance	5
2.1 Introduction	5
2.2 Mechanical model	5
2.2.1 Equation of motion of the individual cyclist	5
2.3 Physiological model.	7
2.3.1 Critical power	7
2.3.2 From critical power to critical velocity	8
2.3.3 Margaria-Morton Physiological Models	8
2.4 Aerodynamic interaction model	10
2.4.1 implementation of drafting	10
2.4.2 Comparison of Aerodynamic interaction studies.	10
2.5 Simulation framework	12
2.5.1 constraints.	12
2.5.2 Strategies	13
2.5.3 Differential equations	14
2.5.4 Solving of differential equations	14
2.6 Cyclists standardisation.	14
2.6.1 Parameters.	14
2.7 Model Sensitivity	15
2.7.1 Mechanical and aerodynamic interaction	16
2.7.2 Physiological.	17
2.8 Validity	17
3 Optimising Strategy	19
3.1 Strategies	19
3.1.1 Regular strategy	19
3.2 Optimisation	21
3.2.1 Objective Function.	21
3.2.2 Separating the Problem	21
3.2.3 Velocity Optimisation	21
3.2.4 Strategy Optimisation	21
3.3 Convergence	23
3.3.1 Elite, mutation and crossover ratio.	23
3.3.2 Population size.	25
3.4 Conclusion	27
4 Analysis of a standard team time trial	29
4.1 Analysis of the regular strategy without workload balancing	29
4.2 Head time optimisation.	30
4.3 Head time optimisation with dropping	30
4.4 Discussion	30
4.5 Conclusion	32
5 Order optimisation	33
5.1 Results	35
5.2 Discussion	35
5.3 Conclusion	37

6	Adjusted Return Positions Strategy	39
6.1	Selected return positions	42
6.1.1	hypotheses.	43
6.2	Results	43
6.3	Discussion	45
6.4	Conclusion	45
7	Skipping Strategy	47
7.1	hypothesis	47
7.2	Results	47
7.3	Discussion	48
7.4	Conclusion	48
8	Conclusion	51
8.1	Model.	51
8.2	Strategy	51
9	Recomendations	53
9.1	Model.	53
9.1.1	Validation of the aerodynamic interaction	53
9.1.2	Individual aerodynamic characteristics	53
9.1.3	Additional aerodynamic improvements	53
9.1.4	Overall performance validation	54
9.2	Studies using the existing model	54
9.2.1	Performance difference on different slopes	54
A	Interpolation of cyclist drafting coefficient	55
A.1	Method	56
A.1.1	Framework.	56
A.1.2	Least squares estimation.	57
A.2	Results	58
A.2.1	interpolation in groups up to eight.	58
A.2.2	Extrapolation from a group of four cyclists.	60
A.3	Discussion	61
A.4	conclusion	61
B	Fitting the Margaria-Morton models	63
B.1	Introduction	63
B.2	The MM-model	63
B.2.1	Differential equations	63
B.2.2	Sizing	65
B.3	Method	66
B.3.1	constraints.	66
B.3.2	Tests	66
B.3.3	Optimisation.	66
B.4	Results and discussion	67
B.5	conclusion	68
	Bibliography	71

Introduction

This report is a study on the optimisation of team time trial strategy, this first paragraph will explain the basics of team time trials in road cycling, after which the details and modelling is described. Team time trials are races in which a team of cyclists compete to finish a predefined course in the lowest amount of time possible. Within the race the cyclists interact with each other, but not with the other teams or other vehicles on the road, thereby making it a team effort. The cyclists are usually with six to eight and drive close after each other to reduce the drag of the cyclists in the tail of the line, this is commonly known as drafting or straying. The cyclists are not allowed to push each other and the drafting effect does not have the same effect in every position in the group, the cyclists change their position throughout the race. A common way to do this is to spend some time in first position, than steer to the side of the group and reduce the power output to move to the tail of the group where, the speed is brought up to the that of the other cyclists until it is possible to pick in to the last position, as demonstrated in figure 1.1. As this repeats each cyclist moves into the front relative to the others, until it reaches the first position and it changes to the last position. It is possible and allowed to use another method to change positions however it is very uncommon.

The full rules of team time trials can e found in the regulation of the ICU [26]. A lot of specific rules can be determined by the organiser of the event. However it is stated that a team time trial should be with at least two and no more than 10 cyclists. The distance of the race should not exceed 100 km, for elite men and 50 km for elite women. The members of the team may use the aerodynamic advantages by drafting from each other, but not from vehicles from the organisation or team support. Neither are teams allowed to draft from other competing teams that are on the same course. There are more rules regarding courses and organisation, but this roughly sketches the outlines of the regulations that affect the strategy.

The goal of this study is to determine performance for different team time trial strategies with respect to each other, in order to try a large amount of strategies a model for simulations is required. This model should model the behaviour of the aerodynamic and physiological behaviour accurately in order to asses the differences between strategies, however it does not necessarily need to exactly match real performance. A mathematical model for the team time trial needs three components: a mechanical of resistance model, a physiological model and an aerodynamic interaction model as illustrated in figure 1.2. The resistances how the power requirements are related to the velocity additionally, it should also include the effects of acceleration and slopes. The physiology should describe the ability of power production, including endurance and intermittent exercise. The modelling of aerodynamic interaction will describe the reductions in aerodynamic resistance, this is important, because the changing of position is a result of the aerodynamic dissimilarities between positions.

The mechanical model links the kinematics to the forces and thereby power output by the cyclist. Many configurations have been used in publications,[3, 12, 14, 15, 18, 23, 24, 36, 38–40, 42, 45, 46] of which «nearly» all of them contain aerodynamic drag and rolling resistance, which are two largest sources of resistance. Some include the forces generated by gravity on sloped roads [18, 23, 24, 36, 40, 45, 46]. Only two studies report the effects of lean on the forward dynamics of the bicycle [39, 45] and the mechanical efficiency of the bicycle is only mentioned in one study [45].

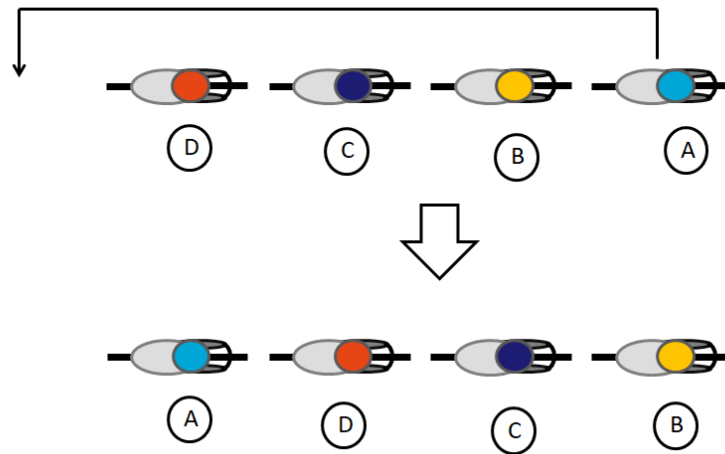


Figure 1.1: Regular changing dynamics in a team time trial of four cyclists. The changing cyclist starts in first position, moves around the group and ends in fourth position.

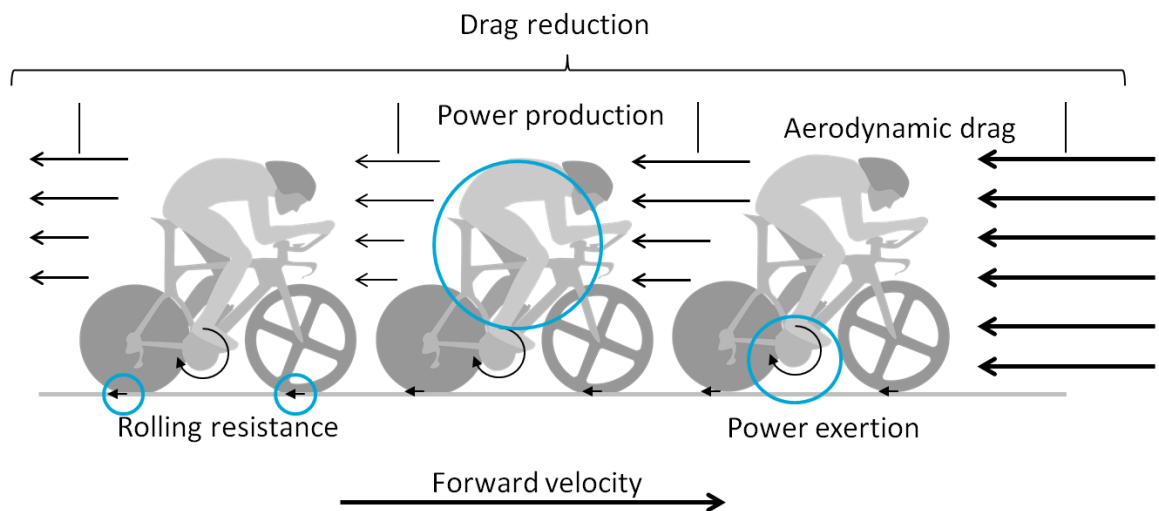


Figure 1.2: An overview of the most important effects to model in a team time trial, resistance (drag and rolling resistance), power production and exertion and aerodynamic drag reduction, spread across three cyclists.

The physiology should provide a mathematical description with on the ability of the cyclist to produce power output over time. Eventually the physiological model should lead to a form in which it can determine whether or not a certain power is producible by the cyclist. The theory of Monod and Scherrer (1965) [30] defines a power to time relationship, more commonly known as the Critical Power Theory. This determines the maximum time a constant power can be delivered by a cyclist. This theory is extended by recovery models of Skiba et al. (2012) [43] and Bartram (2017) [5], creating a model which can model a physiological state (anaerobic work) throughout an exercise, from this state it can be determined if it was possible for the athlete to perform this exercise. Another model is the bioenergetic model by Margaria and Morton [33, 41] (Margaria-Morton model). This model is more based on the bio-chemistry inside the body and also models two physiological states of an athlete, which can determine whether the exercise was possible. The critical power model is easier to determine for a cyclist, with only two variables, the Margaria-Morton model is harder to fit with eight free variables, but is capable of describing a more detailed physiological behaviour of the cyclist.

As mentioned earlier in team time trials drafting is used to increase performance. In order to implement this effect in the team time trial model, the drafting of the cyclists has to be quantified. Several studies have been performed on the drafting effect, when cycling in groups [4, 8, 10, 16–18, 22, 27, 29]. Of these studies four are dedicated to the team pursuit in track cycling and provide data for four cyclists [4, 10, 16, 22] and only two provide data to group sizes up to eight [8, 27]. The discussed studies can also be differentiated by the method of assessment, these are distinguished in three categories: computational flow dynamics (CFD) [8, 16, 27], wind tunnel tests [4, 10] and field tests [10, 17, 22, 29]. These studies describe the drag reduction for every position in the group.

In this study a model will be used in an optimisation to determine optimal strategy in team time trials. As presented in figure 1.1 the strategy that is currently most used is to have a fixed order where every cyclist drives roughly ten to thirty seconds in first position and then changes to last position. In first position the drag is the highest, thus the required power output is high. Depending on the capability of the cyclist and its state at the moment the cyclist will adjust the time spent in that position, shorter if weaker or tired and longer if stronger or in a more energetic state. Cyclists that are much weaker than the others, are often dropped out of the group during the race.

1.1. List of symbols

In table 1.1 a list of symbols used throughout this study is provided.

Table 1.1: List of common symbols used throughout this study

Symbol	Units	Description
ρ	kg/m^3	density
φ	rad	slope angle
A_f	m^2	Frontal area, projected frontal area.
C_{dr}	–	Coefficient of drafting, drag reduction due to drafting
C_d	–	Coefficient of aerodynamic drag
$C_d A$	m^2	Drag area, combination of drag coefficient and corresponding area
C_r	–	Coefficient of rolling resistance
D	N	Drag
F_r	N	Rolling resistance
F_{slope}	N	slope force (projection of gravity on forward direction)
g	m/s^2	gravitational acceleration
\hat{m}_t	kg	total effective mass of bicycle and cyclist
m_b	kg	bicycle mass
m_c	kg	cyclists mass
m_t	kg	total mass of bicycle and cyclist
P	W	power
v	m/s	forward velocity
CP	J	Critical power (CP-model)
W'	J	Anaerobic work capacity (CP-model)
W'_{bal}	J	dynamic anaerobic work capacity state (CP-model)
Φ	-	Relative height of oxidative feed to phosphagen reserve (MM-model)
λ	-	Relative height of connection of glycogen to phosphagen reserve (MM-model)
θ	-	Relative maximum height of glycogen reserve (MM-model)
$D1$	W	Admittance of oxidative feed (MM-model)
$D2$	W	Admittance corresponding to glycolytic production of ATP (MM-model)
$D3$	W	Admittance corresponding to the recovery of glycogen supply (MM-model)
C_P	J	Relative energy capacity of the phosphagen supply (MM-model)
C_G	J	Relative energy capacity of the glycogen supply (MM-model)
E_P	J	Absolute energy capacity of the phosphagen supply (MM-model)
E_G	J	Absolute energy capacity of the glycogen supply (MM-model)

2

Modelling of the team time trial performance

2.1. Introduction

A mathematical model is used to model the physiology of the cyclists during a team time trial. The model is a combination of three models, which are the mechanical, physiological and aerodynamic interaction model. The mechanical model is defined by the equation of motion of the cyclist. The physiological model uses the the cyclists power, from the equation of motion to model the cyclist's physiological state(s). The aerodynamic interaction model is modelled by a constant of drag reduction, this constant can be calculated using the cyclists group positions and aerodynamic drag areas of the cyclists. In this chapter explanations the model, how it is used in simulations, physiological models and aerodynamic models that can be used with this model. A schematic overview is provided in figure 2.1

2.2. Mechanical model

The mechanical model can be described by the equation of motion. In figure 2.2 the free body diagram of the cyclist is considered. Out of plane forces and lean are neglected. The motion of the cyclist is restricted in the vertical direction due to the ground contacts. The equation of motion is defined in this direction. The equation of motion has terms related to slope related forces, rolling resistance, aerodynamic drag and power production by the cyclist. Those last two terms have interaction with the aerodynamic interaction models and physiological models.

A lot of studies have provided a mechanical model that is used to model forces acting on a cyclist. In table 2.1. It is shown that all considered researches consider rolling resistance and aerodynamic drag. Some studies performed an analysis at constant velocity and did not include acceleration. Also a fair amount of studies performed an analysis without road incline and therefore did not include forces as a result of inclination in the road surface. centrifugal forces are not considered much, nor is the chain efficiency.

2.2.1. Equation of motion of the individual cyclist

The equations of motion for the individual cyclist corresponding to figure 2.2. The equation is shown in equation 2.1, the physiological model calculates the time derivative from the current state and the cyclist's power output and the aerodynamic drag reduction coefficient is defined by the aerodynamic interaction model as a function of a cyclist's group position.

$$\frac{P_i}{v_i} = \hat{m}_i \cdot a_i + (mgC_r)_i + \left(\frac{1}{2} \rho C_d A v^2 \right)_i + m_i g \tan(\varphi(x_i)) \quad (2.1)$$

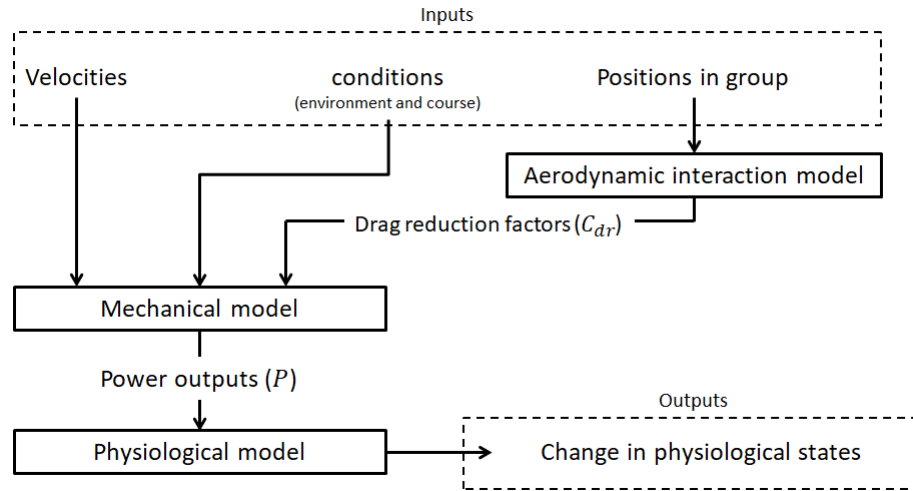


Figure 2.1: A schematic overview of the mathematical model. The inputs are shown at the top and consist of the velocities, conditions and positions of the cyclists in the group. With conditions environmental conditions and course specific parameters are meant. The outputs are the changes in physiological states of all cyclists.

Table 2.1: parts accounted for by different studies that use a mechanical model to address resistances in cycling. The headers of the tabel are abbreviated, Rol = rolling resistance, Acc = acceleration, Grad = forces introduced by gravity and road inclination, Centripetal = (lateral) centripetal forces, Efficiency = efficiency of the chaindrive

Study	Effects modelled					
	Drag	Rolling	Acc	Grad	Centripetal	Efficiency
Candau et al. (1997) [11]	x	x				
Baldisera (2017) [3]	x	x				
de Koning et al (1999) [14]	x	x	x			
Debraux et al (2011) [15]	x	x				
di Prampero et al (1979) [40]	x	x		x		
di Prampero (2000) [39]	x	x	x	x	x	
Fitton et al. (2018) [18]	x	x	x	x		
Gordon (2005) [42]	x	x				
Hennekam and Botsema (1991) [23]	x	x	x			
Hettinga et al. (2012) [24]	x	x	x			
Olds et al. (1993) [36]	x	x	x	x		
Padilla et al (2000) [38]	x	x				
Underwood and Jeremy (2010) [45]	x	x	x	x	x	x
Van Ingen Schenau and Cavanagh (1990) [46]	x	x	x	x		

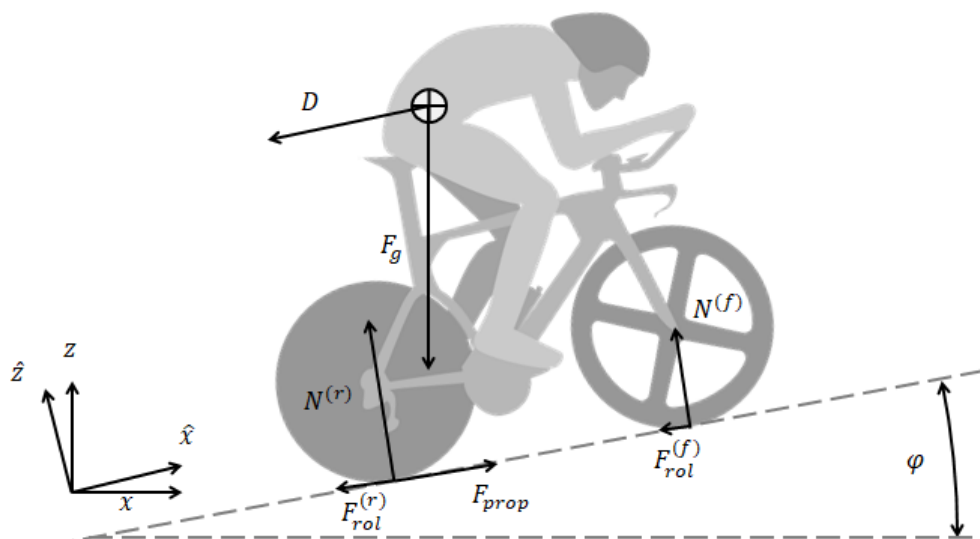


Figure 2.2: A free body diagram of the cyclist and bicycle combination.

2.3. Physiological model

The physiology is an important part of the model, with the physiological model it is determined if the physiological effort of producing the power is achievable. The physiological models derive the states from the power output over the team time trial. The power effectively defines the derivative of the physiological state(s) of the cyclist, which result in the physiological states by forward integration. Multiple physiological models are used in this study.

Different models Different models can be used to model physiological performance, the two models used in this study are the critical power model and Margaria-Morton whole-body bioenergetic models. The critical power model is mostly used in cycling performance modelling, since the tests to obtain the cyclists specific values are relatively easy. [2, 6, 7, 25, 35, 47, 48] With this model multiple recovery methods have been proposed [5, 34, 43], where the model by Bartram seems to fit best for elite cyclists and therefore is used as the recovery model with the CP-model[5]. Another physiological model is provided by Margaria and Morton [33, 41], this model is based on the biochemistry involved in mechanical power production. This model therefore models the performance, more detailed. Because of it's detail it is hard to fit such model to a cyclist, no publications have been found doing so. From it's degrees of freedom it is however derived that at least eight tests are required.

2.3.1. Critical power

The critical power model by Monod and Scherrer (1965) [30] is based on a mathematical relationship between exercise power and duration. According to the model each cyclists has a critical power (CP) which the cyclist is able to sustain for a very long time, this corresponds to aerobic power production. When producing above this power, a limited capacity of anaerobic work (W'). The average power over an exercise is shown in equation 2.2, where t_{lim} is the duration of the exercise.

$$P_{lim} = CP + \frac{W'}{t_{lim}} \quad (2.2)$$

$$W_{max} = CP \cdot t_{lim} + W' \quad (2.3)$$

The dynamical state of the anaerobic work capacity is defined by W'_{bal} , during a depletion of the anaerobic reserve the change of the state of anaerobic work capacity is the amount of power delivered above the critical power, see equation 2.4. By integrating this over an exercise duration (t_{lim}) using any power (P_{lim}) larger than CP, the original relation from equation 2.3 is obtained, thus this equation satisfies the original model. The original model only models the expenditure and not the recovery. [30, 32]

$$\frac{dW'_{bal}}{dt} = CP - P \quad P > CP \quad (2.4)$$

Bartram's recovery model [5] The recovery of Bartram's model is modelled as a first order differential equation, based on the theories of Skiba et al (2012) [43] and Morton and Billat (2004) [34]. This first order differential equation equation 2.5a has one parameter corresponding to the refill rate (τ), this time constant is modelled as a function of recovery power $Dcp = CP - P$, see equation 2.5b. This equation is fitted to tests performed by elite cyclists.

$$\frac{dW'_{bal}}{dt} = \frac{W' - W'_{bal}}{\tau} \quad CP > P \quad (2.5a)$$

$$\tau = 2287.2 \cdot (CP - P)^{-0.688} \quad (2.5b)$$

Skiba's recovery model [43] The recovery model by Skiba is most standard in physiological modelling, however there are some conflicting things on this model. First of all the recovery equation reported by Skiba et al (2012) [43] contains an equation where it's units mismatch and also does not correspond to the behaviour shown, this equation is slightly altered, such that the behaviour corresponds and the units match. An additional point is that when the power output approaches critical power, the recovery rate does not approach zero, which result in that a slightly varying power output around CP has a much higher performance, thus also resulting that the accuracy of determining the CP is corrupted. At last the model is not fitted to a cycling test or tested with elite athletes, which makes it less useful with respect to the Bartram Model.

The model itself is based on the recovery kinetics proposed by Morton and Billat (2004) [34], with the equation shown in equation 2.6a. Just as in Bartram's model the time constant τ is fitted as a function of the recovery power: equation 2.6b.

$$\frac{dW'_{bal}}{dt} = \frac{W' - W'_{bal}}{\tau} \quad CP > P \quad (2.6a)$$

$$\tau = 546e^{-0.01 \cdot (CP - P)} + 316 \quad (2.6b)$$

2.3.2. From critical power to critical velocity

Using the mechanical model the critical power can directly be linked to a velocity, at critical power this value is defined as the critical velocity (CV). The critical velocity is, a velocity that can be maintained for a long time. This variable is influenced by environmental parameters (ρ , φ) and cyclist or bicycle parameters (C_r , $C_d A$). The critical velocity can be useful in determining the group velocity during a team time trial.

2.3.3. Margaria-Morton Physiological Models

The Margaria-Morton models are based on physiological processes in the body rather than mathematical relations found in tests. These models are mostly used to explain phenomena in exercises. [33, 41] These models could also be fitted to athletes.

Instead of one aerobic capacity as described in the critical power model, this model has two anaerobic capacities. The first anaerobic capacity is related to the bodies capacity of phosphates, used in the production of ATP, which is directly used in production of mechanical work by the muscles. The second anaerobic capacity is related to the supply of sugars in the form of lactate or glycogen, this reacts much slower than the phosphates. Another component in this process is the aerobic feed of energy, which contributes to the continues refilling of both anaerobic capacities.

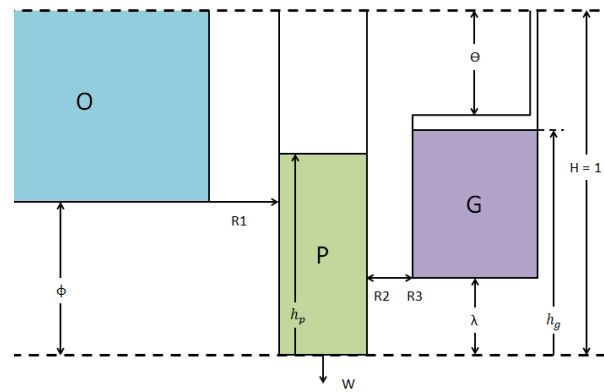


Figure 2.3: Hydraulic flow representation of the generalised MM model.

A schematic hydraulic flow model is presented in 2.3. In this model the volume flow rates represent energy flows and the capacities energies. The P tank represents the potential energy production of phosphates. The G tank represents the energy potential of stored glycogen (or lactates?). The O tank represents oxygen supply which is taken from the environment and therefore infinite in capacity, but limited in feed. The power output is directly depletes the P tank, the level difference created by depletion causes flows from O and G tank to the P tank. The flow from P to G, representing recovery of glycogen, is much slower than the flow in opposite direction.

This model models the flow of energy inside the athletes body more accurate than the critical power model, however a lot of parameters of this model are required to use this model in predictive modelling. Little information has been published on how to fit a such a model to an athlete and the constraints to the parameters. [31]

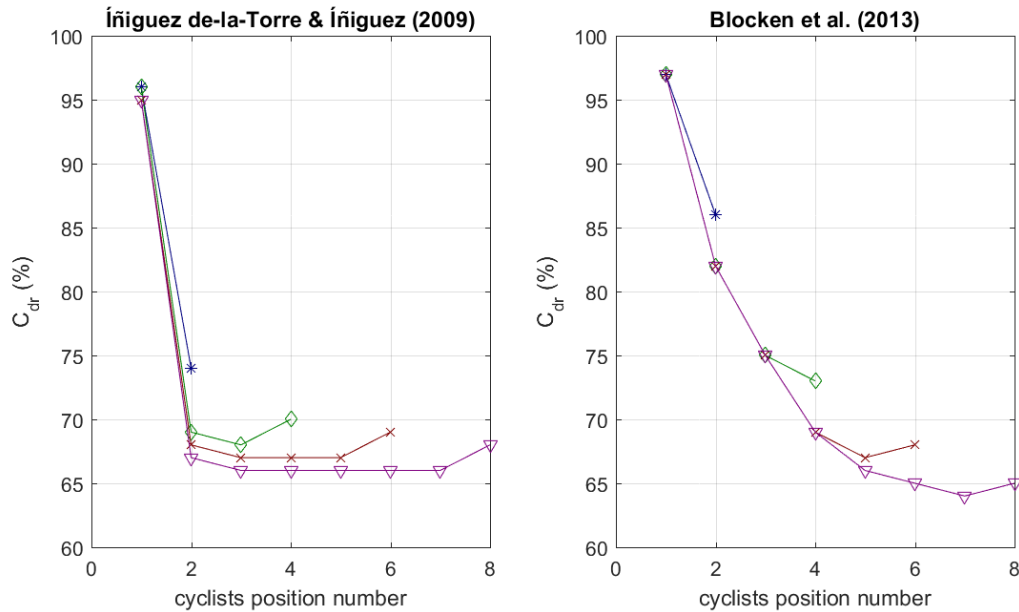


Figure 2.4: The drafting coefficients versus the position in the group for multiple group sizes (2,4,6 and 8). The left plot corresponds to Íñiguez & Íñiguez de-la-Torre [27], the right plot corresponds to Blocken. [8] The two studies both present data that is

2.4. Aerodynamic interaction model

In the aerodynamic interaction model the drafting is modelled. Several studies tried to model the aerodynamic interaction by means of CFD simulations [8, 16, 27], wind tunnel tests [4, 10] and field test using bicycle mounted power meters [10, 18, 22]. Only two studies have been

2.4.1. implementation of drafting

In order to account for drafting in the equation of motion therefore the formulation from [29] is used, expressed in equation 2.7a. Another way of approaching this is by assuming that the cyclists effective air velocity is reduced by the other cyclists, this results in equation 2.7b.

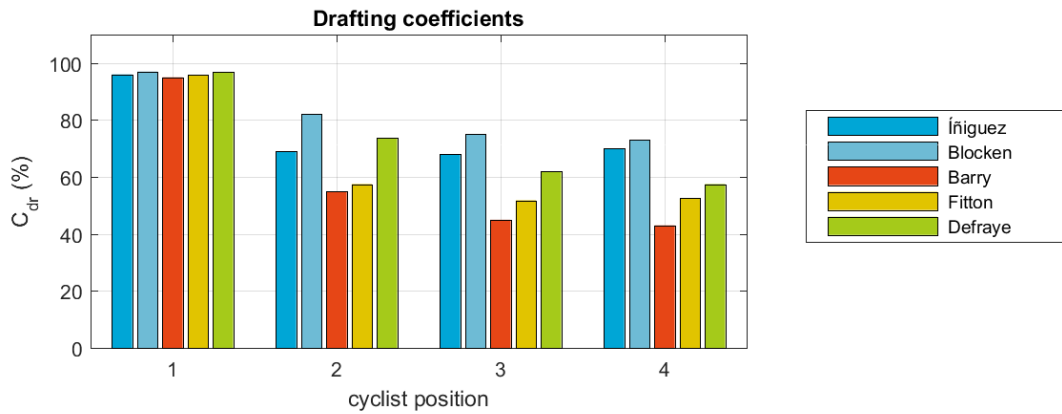
$$D = \frac{1}{2} \rho C_{dr} C_d A v^2 \quad (2.7a)$$

$$D = \frac{1}{2} \rho C_d A v_e^2 \quad v_e^2 = C_{dr} v^2 \quad (2.7b)$$

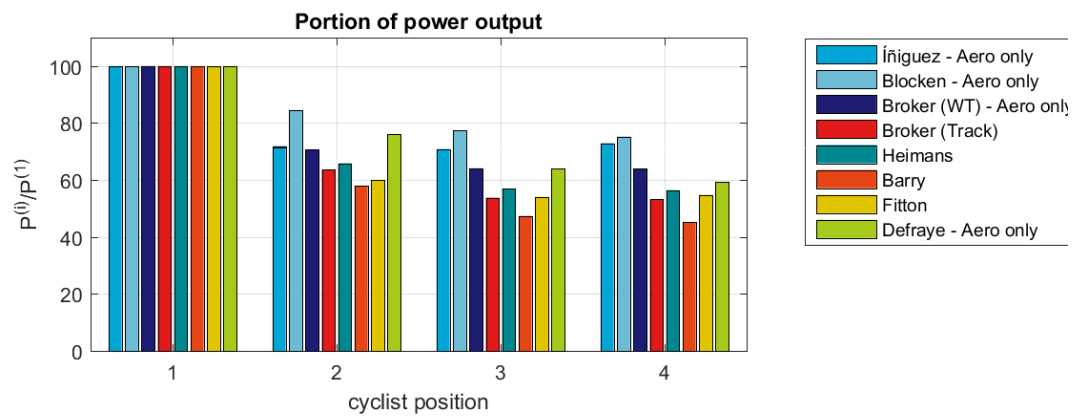
2.4.2. Comparison of Aerodynamic interaction studies

Two aerodynamic drag reduction studies are performed on groups of cyclists with up to eight cyclist [8, 27], more studies are used to determine drag reductions in groups of four cyclists. [4, 10, 16, 18, 22, 29] The two studies reporting drag reduction of groups up to 8 cyclists show different behaviours for the development of drag reduction through the positions of cyclists in the group, see 2.4. A comparison of the drafting coefficient in groups of four cyclists are shown in 2.5a, where the first two bars in each position represent the results from Íñiguez and Blocken.

Observing groups of four cyclists When observing 2.5a, it is found that the three studies, which are not able to model eight cyclist show lower values, in the last two positions. Especially the studies of Fitton [18] and Barry [4] which use field tests and wind tunnel tests respectively, where Defraye [16] also uses CFD. Wind tunnel tests and even more field tests are a more representative study of drag, therefore also drag reduction. This makes it very likely that coefficients of drafting are lower (drag reduction is higher) than both Blocken [8] and Íñiguez [27] report.



(a) Comparison of drag reduction coefficient (C_{dr}) as function of group position coefficient for groups of four cyclists.



(b) Comparison of drag reduction, in terms of ratio in power consumption with respect to the first cyclist in the group, as function of group position coefficient for groups of four cyclists.

Figure 2.5: Comparison of drag reduction of groups of four cyclists.

Drafting values The drafting values of all studies are compared. In figure 2.4 the drafting coefficients for groups of two, four, six and eight cyclists are compared between the two studies simulating groups up to eight cyclists. [8, 27] The values used in these studies are shown in table 2.2 for Íñiguez & Íñiguez de-la-Torre [27] and in table A.2 for Blocken et al. [8]. The data from groups of three, five and seven cyclists was not provided by the study of Blocken et al. [8], therefore these values were interpolated. The method of interpolation is explained in appendix A. In this chapter also an attempt is provided to use groups of four cyclist to extrapolate their values, however the analysis showed that the interaction over more than 3 positions is to high to neglect. This leads to the need of fitting a wake function, in order to extrapolate drag reduction in groups of four cyclists.

Table 2.2: Drafting coefficients as reported by Íñiguez & Íñiguez de-la-Torre

Gr. Size	C_{dr1}	C_{dr2}	C_{dr3}	C_{dr4}	C_{dr5}	C_{dr6}	C_{dr7}	C_{dr8}
1	100							
2	96	74						
3	96	71	72					
4	96	69	68	70				
5	95	68	67	67	69			
6	95	68	67	67	67	69		
7	95	67	66	66	66	66	68	
8	95	67	66	66	66	66	66	68

Drafting coefficients, expressed as the percentage of the drafting drag value of the original solo drag value.

Table 2.3: Drafting coefficients as reported by Blocken et al. with groups of 3, 5 and 7 interpolated using the alortighm form (refCorrec-Appendix)

Gr. Size	C_{dr1}	C_{dr2}	C_{dr3}	C_{dr4}	C_{dr5}	C_{dr6}	C_{dr7}	C_{dr8}
1	100							
2	97	86						
3	97	83	78					
4	97	82	75	73				
5	96	82	75	70	69			
6	97	82	75	69	67	68		
7	96	82	75	70	66	66	66	
8	97	82	75	65	66	65	64	65

Drafting coefficients, expressed as the percentage of the drafting drag value of the original solo drag value.

2.5. Simulation framework

The goal of the simulation is to assess the performance of a strategy. The strategy is simulated up to the point where either the physiological states get out of their bounds, or enough cyclists have finished. The equations of motion are used to determine the power output of the cyclists, this is used by the physiological model to calculate the physiological states. The physiological states by themselves can show a lot about the workload relative distribution during the team time trial, but more important is to define, weather or not the simulated condition is actually achievable. From the simulation the finish time is used to determine the performance. In case of a physiological failure, another method is used to come to a finish time.

2.5.1. constraints

The goal of the simulation is to obtain the physiological states of a cyclist during a team time trial, this means that all other free variables have to be pre-defined. The cyclists travel over the course, the three dimensional environment is brought down to just one free coordinate, distance (s). The position on the map, height and slope are all a function of the distance coordinate, and corresponding to a specified course.

In a real course there will very likely be turns, roundabouts and possibly speed bumps that affect the strategy of a team time trial, however these effects are neglected in this study. In turns the travelling velocity is limited and changing position is harder or not possible, these effects could be useful when preparing for a real team time trial, however in this study races without course constraints are simulated.

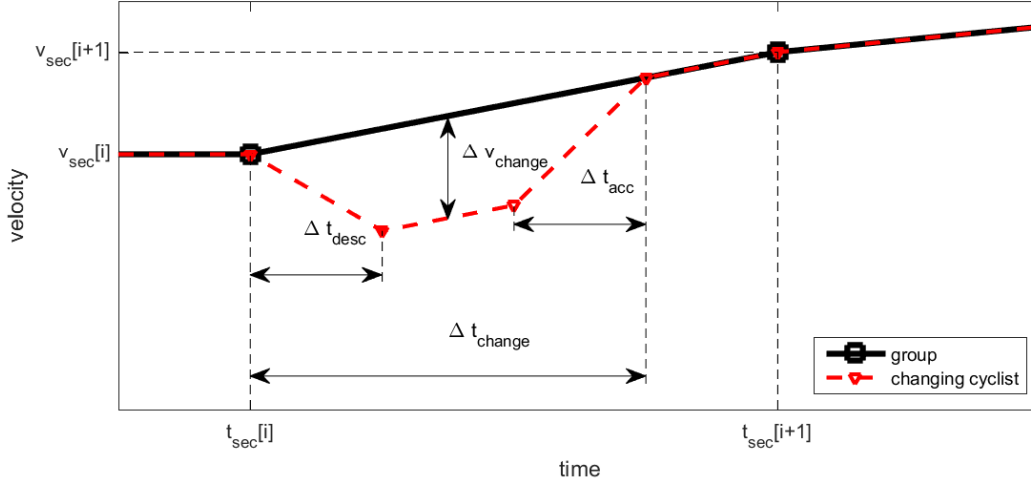


Figure 2.6: The velocity profile and definition of section velocity

2.5.2. Strategies

With the strategy is determined as a function of time, what the positions are as a function of time, also the group velocity is determined and the time it takes to change position. The velocity of the group can vary from section to section and is specified at the point of change in position. The position is integrated from velocity during the simulation, the velocity and accelerations of individual cyclists is determined by whether or not the cyclist is in the group or changing. In the group the velocity and accelerations of all cyclists are equal, the velocity is linear interpolated between the values at the beginning of the section.

Velocity of changing cyclist The velocity of the changing cyclist is determined from the distance from between the old and new positions and the time of changing. A plot is made with the velocities of both group and changing cyclist and is shown in 2.6, with the corresponding equations in equation 2.8. The section velocity $v_{sec}[i]$ is the velocity at the beginning of section i . The velocity profile of the changing cyclist is characterised by three phases, first is the decelerating phase, second is the constant velocity phase and last is the accelerating phase. During the accelerative and decelerating phase, the acceleration, with respect to the group (Δa), is set to $0.2m/s^2$ and is negative during decelerating phase and positive in acceleration phase. The duration of changing (Δt_{change}) is also specified, the velocity difference is matched such that the cyclist ends in the correct position, see equation 2.9. Since the velocity in begin and end are equal to the group velocity, the acceleration and deceleration phase need to be of the same length and are defined by equation 2.10.

$$v_{change}(t) = \begin{cases} v_{group}(t) - \Delta a \cdot (t - t_{sec}[i]), & t_{sec}[i] \leq t < t_{sec}[i] + \Delta t_{dec} \\ v_{group}(t) - \Delta v_{change}, & t_{sec}[i] + \Delta t_{dec} < t \leq t_{sec}[i] + \Delta t_{change} - \Delta t_{acc} \\ v_{group}(t) + \Delta a \cdot (t_{sec}[i] + \Delta t_{change} - t), & t_{sec}[i] + \Delta t_{change} - \Delta t_{acc} \leq t \leq t_{sec}[i] + \Delta t_{changing} \end{cases} \quad (2.8)$$

$$\begin{aligned} \Delta S &= \int (v_{change}(t) - v_{group}(t)) dt \\ &= \Delta v_{change} - a \cdot \Delta t_{dec} - a \cdot \Delta t_{acc} \end{aligned} \quad (2.9)$$

$$\Delta t_{acc} = \Delta t_{dec} = \frac{\Delta v_{change}}{a} \quad (2.10)$$

Drift correction Because of the forward integration a drift is introduced, which is partially corrected for this effect originates from the conversion of continuous functions to discrete data sets. All integrated variables are effected by this effect. During the simulations for the most part velocity is prescribed, because a fixed

time step was used the accelerations can be calculated from this prescribed velocity. The velocity only deviates from the prescribed velocity, when cyclists are dropped out of the group. The velocity integrated from the acceleration is used rather than the prescribed velocity because this will effect the energy balance, between mechanical work performed by the cyclist and the kinetic energy. The accelerating and de-accelerating phases in the changing procedure will be exactly of exactly the same duration and therefore the velocity will not have any drift due to this procedure, the distance is slightly effected. Therefore the cyclist will be of from the aimed position after changing. Since the spacing between cyclist should be fixed, when in formation, the drift can be corrected for the cyclists right after the changing procedure is performed. This is done by adding a peak in the velocity profile, which corrects the distance with respect to the others.

2.5.3. Differential equations

The set differential equations can be defined as a function that calculates the state derivative with respect to time as a function of the state and the time. The state contains all the variables which are integrated. Since the simulation contains multiple cyclists the states of all cyclist. The mechanical model has the travelled distance (s) and velocity (v) as states. The critical power model has the dynamic anaerobic work capacity (W'_{bal}) and the Margaria-Morton model has the two energy levels (h_P and h_G) as states.

2.5.4. Solving of differential equations

The differential equation is solved using an euler integration scheme. The state denoted with \mathbf{X} contains position data as well as the physiological states. The physiological states, velocity and position of all cyclists. Only the group velocity is predefined, so not individual velocities and acceleration, those are calculated in the same process as the physiological state differences. The difference in physiological state, acceleration and velocity are de state derivatives. The states are determined by numerical integration using Euler integration scheme as shown in equation 2.11. Here \mathbf{X}_i is the current state, \mathbf{X}_{i+1} the next state and Δt_i the time step.

$$\mathbf{X}_{i+1} = \mathbf{X}_i + \frac{d\mathbf{X}_i}{dt} \cdot \Delta t_i \quad (2.11)$$

The usage of more accurate and complex solvers were considered. For example a fourth order Runge-Kutta solver is likely to give a much more accurate integration. The simulation as it is, has lots of logical stage switches which are harder to implement while using higher order solvers. The way it is programmed is that there are numerous variables called from the integration loop that are not stored in the states, therefore the state derivatives are not a function of only time and state, which makes it harder to use higher order solvers. It must also be noted that between the compared simulations the changing behaviour is more or less equal, accelerations and durations of changing are kept equal between simulations, therefore a small integration error will be present in both of the compared simulations and thereby not influence the results.

2.6. Cyclists standardisation

During this report standardised cyclists will be representing varying cyclists performance characteristics in a team. Team time trials are often a part of a multiple stage event meaning that, the cyclists selected will likely vary in performance characteristics. The results of this study are generated by using parameters for standardised cyclists. The parameters associated with these standards as well as a performance comparison is discussed.

2.6.1. Parameters

The standardisation of cyclists is split up into two categories, the mechanical standards and the physiological standard. Within the physiological standards there are of course two types, corresponding to critical power and Margaria-Morton models. The mechanical standards are the masses and coefficients of resistance. The standardisation for mechanical coefficients is done per weight class (heavy, medium or light). The physiological parameters are split into classes of power output (super strong, strong, medium, weak).

Mechanical standards

Within the mechanical constants some vary per class and others are independent, the varying parameters are cyclist mass and drag area, the others are the same for all cyclists. The three classes correspond to a body

mass (m_c), heavy (80 kg), medium (70 kg) and light (60 kg). Heil (2002) [21] made an estimation of frontal area of a cyclist with respect to the body mass independent of length, this scaling is used to scale the drag area with the masses, neglecting change in drag coefficient. The drag area was assumed to be $0.22m^2$ for the medium cyclist and scaled to the heavy and light cyclist. The coefficient of rolling resistance (C_r) is taken from the Vittoria Corsa Speed tires tested by [1] at an inflation pressure of 8.3 Bar. The bicycle mass is taken from Team Sunweb's time trial bicycles, the Giant Trinity Advanced Pro TT. Table 2.4 shows the parameters for the cyclists' weight classes.

Table 2.4: Standardised mechanical coefficients in weight classes.

Weight class (-)	m_c kg	m_b kg	\hat{m}_t kg	C_r -	$C_d A$ m^2
Heavy	80	8.7	90	0.0027	0.24
Medium	70	8.7	80	0.0027	0.22
Light	60	8.7	70	0.0027	0.20

Physiological CP standards

For the cyclists standardisation, the critical power is varied in steps of $30W$ over four categories, the anaerobic capacity is scaled proportional with the critical power. This way if a power output is considered which is a proportion of the critical power above the critical power, the time to exhaustion is equal for all cyclists. The recovery is done by either Bartram's [5] model, which do not require cyclist specific parameters. The results are shown in table 2.5.

Table 2.5: Standardised physiological coefficients in strength classes for the CP-model.

Power class ()	CP W	W' kJ
Super strong	450	25.0
Strong	420	23.3
Medium	390	21.7
Weak	360	20.0

Physiological MM standards

The MM-model coefficients are fitted to their CP-model counterparts, the full method and analysis can be found in B. The MM-model is with assumptions fitted to the outcomes of four tests which were generated by simulations using the CP-model. Of the four tests, two were related to endurance and one to intermittent exercise. It is argued that a more realistic result could be found if the model was fitted to real athletes.

Table 2.6: Standardised physiological coefficients in strength classes for the CP-model.

parameter	units	Weak	Medium	Strong	Super Strong
Φ	-	0.2	0.2	0.2	0.2
λ	-	0.1	0.1	0.1	0.1
θ	-	0.4	0.4	0.4	0.4
$D1 = R1^{-1}$	W	461.7	500.1	538.6	577.1
$D2 = R2^{-1}$	W	1290	1398	1505	1613
$D3 = R3^{-1}$	W	960.0	1040	1120	1200
C_P	kJ	10.00	10.83	11.67	12.50
C_G	kJ	72.72	78.78	84.84	90.90

2.7. Model Sensitivity

With the sensitivity analysis the influence of an individual cyclist's mechanical, physiological and aerodynamic parameters as well as environmental parameters are assessed. In this analysis no simulations are used to eliminate the effects different strategies might have. The team time trial performance is in large extent dependent on the individuals' critical velocities. Which is the velocity corresponding to the critical power and can be maintained until fatigue will arise, which is after around 40 minutes [28].

2.7.1. Mechanical and aerodynamic interaction

From the equation of motion the critical velocity is determined, the change in critical velocity resulted by the change of a parameter by 1 % determines the sensitivity of that parameter. The equation of motion is written in a polynomial form, from which the critical velocity (2.12). Since the equation is a third order polynomial function there will be three solution, however only one of the solutions found is a real number, this is the solution that is used.

$$m_t \cdot g \cdot (C_r + \sin \varphi) \cdot CV + \frac{1}{2} \rho C_{dr} C_d A CV^3 - CP = 0 \quad (2.12)$$

$$S_{par} = \frac{\delta CV}{CV} \quad (2.13)$$

The method for determining the influences in power, can be determined for various conditions. Three conditions have been chosen, the first is a solo cyclist on flat terrain. The second is a cyclist in a group with a drafting coefficient of 78 %, corresponding to the third position, by Blocken's model [8], also on flat terrain. The third is a solo cyclist on a slope of 3 degrees (5.2 %). The cyclist considered is a strong, medium weight standardised cyclist and all situations are modelled at critical velocity (CV), which is the velocity corresponding to $P = CP$. All parameters are shown in table 2.7 and the results of variation tests are shown in table 2.8. The influence is given as a percentage increase in critical velocity, as an effect of the increase by 1 % of the considered parameter.

Table 2.7: The parameters used in the variation cases

Parameter	Units	case 1	case 2	case 3
Strength class	-	Strong ($CP = 420$)	Strong ($CP = 420$)	Strong ($CP = 420$)
m_c	kg	70	70	70
m_b	kg	8.7	8.7	8.7
m_t	kg	78.7	78.7	78.7
C_r	-	0.0027	0.0027	0.0027
φ	deg	0	0	3
C_{dr}	-	1	0.78	1
$C_d A$	m^2	0.22	0.22	0.22
v	m/s	14.25	70	3.72
g	m/s^2	9.81	9.81	9.81
ρ	kg/m^3	1.225	1.225	1.225

Table 2.8: The results of the variation tests, values correspond to the change in power per percent change in the constant with respect to the original value.

parameter	Influence case 1	Influence case 2	Influence case 3
CV	14.25 m/s	15.45 m/s	3.720 m/s
m_c	-0.00270%	-0.00300%	-0.0676%
m_b	-0.0220%	-0.0240%	-0.543%
C_r	-0.0247%	-0.0269%	-0.0300%
φ	0.00%	0.00%	-0.580%
ρ	-0.323%	-0.114%	-0.129%
C_{dr}	-0.323%	-0.114%	-0.129%
$C_d A$	-0.323%	-0.114%	-0.129%

discussion The sensitivity of the mechanical model is assessed the sensitivities found vary a lot between the cases. On flat terrain (case 1 and case 2) the parameters corresponding to drag (ρ , C_{dr} , $C_d A$) are high in sensitivity. Also the velocity is high, meaning that much more power is required with a slight increase of velocity, in other words by applying more power the velocity will only rise slightly. In the flat terrain cases the masses do not have a large influence. In the third case, where there course is 3 deg uphill, the masses have a much larger role with respect to the aero dynamic variables, also the terrain has a high sensitivity. In absolute

values the slope angle has an equal sensitivity in both cases, only the rise of one percent of the original value is zero for the first two cases (since the value is zero). The rolling resistance does not have a high sensitivity in any of these cases.

2.7.2. Physiological

In order to assess the sensitivity of the physiological model, the change in mean power output of the cyclists is studied. The simulation consists of a 10 km flat team time trial, where the group velocity is optimised for the lowest end time as described in 3.2.3. Each physiological variable for both CP-model and MM-model is varied individually and the results are compared. The influence on performance is expressed in mean power over all cyclist over the whole race. The simulation was performed with a group of eight cyclists of strength class medium. The changing scheme was set such that each ten seconds a cyclist changed in 1 seconds from first to last position. The results are shown in 2.9. The first column shows the parameter, the second column shows the value from which is evaluated and the third shows the relative increase in power as a function of the 1 % increment in parameter.

Table 2.9: The results of the variation tests, values correspond to the change in power per percent change in the constant with respect to the original value.

varied parameter	Base value	Influence on power
CP	390W	0.893%
W'	21.7kJ	0.130%
Φ	0.2	-0.113%
λ	0.1	-0.0278%
θ	0.4	-0.0095%
D1	500.1W	0.85%
D2	1398W	0.0042%
D3	1040W	0.0025%
C_P	10.83kJ	0.0488%
C_G	78.78kJ	0.349%

Discussion CP The results in 2.9 show that for the CP-model the critical power is more influential to performance than the anaerobic capacity. The influence of CP to the power is about seven times the influence of W', this can be explained by the power profile of the team time trial. The team time trial is an intermittent exercise, increasing the CP will result in more or longer recovery phases, more recovery and less depletion of the anaerobic reserve in expenditure phases. Increasing the W' will only increase the endurance in expenditure phases and increase recovery.

Discussion MM Within the MM-parameters, the parameter D1 is most influential to mean power output, as can be seen in 2.9. Within the admittances to the power flows D1 is far larger than the other two, the parameter D1 is just as CP from the CP-model related to aerobic power production. Also within the relative sizing constants (Φ , λ and θ), the one related to aerobic power production (Φ) is the most influential. Also with this model the effect of the size of anaerobic capacity is little with respect to the influence of constants related to aerobic power production

Conclusion Constants related to the production of aerobic power are most influential to the mean power production of a team time trial. Comparing these the influence of the mechanical parameters on the power consumption, it can be concluded that the constants related to aerobic power production are about as influential as aerodynamic parameters in flat team time trials and more influential than mass and slope parameters in team time trials with gradients smaller than 5.2 %.

2.8. Validity

This model still lacks in validity This is mainly because the used aerodynamic interaction coefficients are not reproduced during a track test. Drag reduction values of groups with a maximum of four cyclists are reported, but unusable since this study specifically evaluates team time trials in road cycling in which coefficients of groups up to eight cyclists are required.

One way to improve the validity of the model presented in this study is to improve the validity drag reduction coefficients. This can be done by reproducing the values from the CFD tests in a track test, as are performed on groups of four cyclists [10, 18, 22].

Another way to increase the validity is to simulate a strategy that was performed in a real race. For example the velocity could be optimised while maintaining the same changing scheme in order to assess the best achievable finish time given the strategy and compare this to the performed result. However in order to do this, for a group of cyclists both a physiological model has to be fitted and aerodynamic drag area of all cyclists has to be determined accurately.

3

Optimising Strategy

The strategy of a team time trial can be described by a lot of parameters. The most defining are the times spend in positions and the positions of cyclists over time. Different less important parameters are the change duration and the acceleration and deceleration while changing. Alternatively the wheel gaps and lateral deviations can be modelled, however the current model is unfit to do so since there is no data on the change of aerodynamic drafting coefficients as a function of these parameters is undefined. In this study only the main parameters, cyclists positions and times spend in positions are assessed in later studies it is also possible to vary the other parameters.

3.1. Strategies

As explained in chapter 2 the strategy is the description of the cyclists position in the group, change duration, velocity during the race. For each different section, where the cyclists have the same position in the group, including the part where the cyclists change their position; the strategy contains their velocity, the time it should take to perform the change their position, and the positions of all cyclists and the time the start time of this configuration. For a 40 minute race with eight cyclist where the cyclists keep their formation over 20 s this yields 120 formations, leading to 1320 free variables. In real races strategies are simplified by a set of rules to make the strategy less complex, for example always change from first to last position, or when tired reduce time in first position. In this section the strategies will be explained and how they are optimised.

3.1.1. Regular strategy

The most regular strategy is used as the baseline in this study, it is performed by many teams in professional road cycling. The team starts in a predefined order. Changing happens from first to last position, where all other cyclist effectively shift one position forward, due to the absence of the previously first cyclist in group, see figure 3.2. To differ the workload between cyclists in a team, the time for each cyclist in first position (head time) is varied among the cyclists.

Using the regular strategy the number of free variables is reduced. Using the previous example of a 40 minute race, the positioning options has been reduced by a factor 120 ($8 \cdot 120$ to 8) and the time of changing options by a factor 15 (120 to 8). The group velocity can be defined by sections of the course, or made as a function of the courses slope. This leads to a strategy that has two free parameters per cyclist with additional velocity parameters.

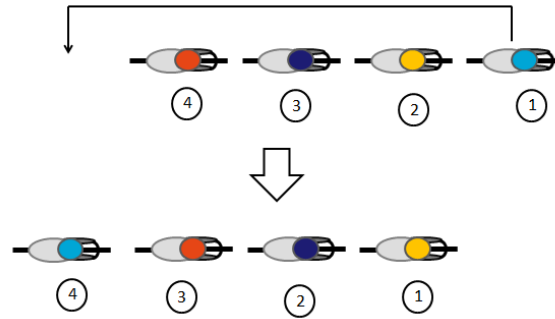


Figure 3.1: A position change according to the regular strategy, the circled numbers denote the group position of the cyclists. The cyclist in first position changes to the last position, therefore all other cyclists shift to one position in front.

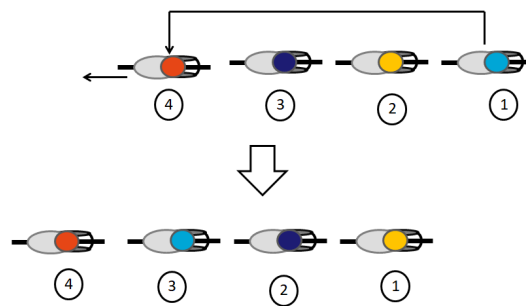


Figure 3.2: A position change according to the variable return position strategy, the circled numbers denote the group position of the cyclists. In this case the cyclist first position goes to the third position, the cyclist in position four remains in position four, but will have to make room for to let the cyclist in third position, the cyclist in position two and three become the cyclists in position one and two respectively, but keep their velocity constant.

3.2. Optimisation

Optimisations can be performed to estimate the optimal inputs to a strategy. For each strategy inputs can be defined, such as initial positions, head times or velocity. The optimisation uses an objective function to determine a score, this score is minimised by altering the inputs to the objective function, such that the score will be lowest. In the optimisations in this study the score is the finish time of a team time trial, which is the time in which four cyclists pass the finish line. For applicability the values are presented as the average velocity over the race, which is computed by dividing the race distance by the finish time.

3.2.1. Objective Function

To optimise performance an objective function is used, this function gives a score to the strategy, which is minimised. The objective function is the simulation, the finish time is used as the objective value, therefore an performance optimisation will always optimise towards a lower finish time, if the optimisation is convergent. It could be that one of the cyclists fails to execute prescribed strategy, in this case the simulation is terminated. To compute the finish time in cases of physiological failure, it is assumed that the cyclists are able to complete the race by cycling at a velocity of 30 km/h. This velocity is used to compute the time required to complete the maintaining distance and added to the time of failure. This "motivates" the optimisation to move the moment of failure towards the finish, for a better convergence.

3.2.2. Separating the Problem

The free variables of a strategy are composed of two types, the continuous variables and the integer constraint variables. The continuous variables in this problem are the velocities of sections of the race. The integer constraint variables are the initial positions, the return positions and the head times. The head times could also be presented as continuous numbers, however they are set in steps of 10 seconds to reduce the size of the problem. To asses a strategy the velocities are not provided as inputs, but optimised at each iteration of the strategy optimisation. This is done to improve the convergence of the problem.

3.2.3. Velocity Optimisation

For each strategy in the optimisation, the velocity is optimised to give maximum result over the simulation, given the specified strategy. The strategy could contain multiple velocities, for example when the slope varies along the course, different sections will have most likely have different ideal velocities, therefore the velocity is a multiple input, single output optimisation.

The algorithm used for the velocity optimisation is the derivative free method. This method is chosen because the velocity optimisation has both continuous input (velocity) and continuous output, from which a gradient can be computed. The algorithm is set to optimise until the input velocity difference is lower than 0.005 m/s.

3.2.4. Strategy Optimisation

Genetic algorithm is used to optimise strategy since it is able to handle problems with many local minima and integer constraints and is still able to find the global minimum. The strategy parameters that were varied in this study are, initial positions, times spend in first position, and «return position», of which only the times spend in first position are continuous. Since the interest is in the global optimum and not the local optima, the are also discretized to steps of 10 seconds.

The genetic algorithm uses an evolution inspired method of crossing and mutating bit strings that contain the inputs of the objective function. The population size determines how many sets of bit strings are considered in each generation. The input of the genetic algorithm is converted to a bit string, the length of the bit string defines the complexity of the problem. The higher the complexity the lower the convergence rate, meaning a larger population size and/or number of generations is needed to achieve the same accuracy. The optimisation of different strategies require different inputs. These inputs are if necessary discretized. The complexity of the inputs are listed below. Note that all numbers have to be rounded upwards.

- Order: The order is selected from a list of all possible orders depending on the number of cyclists (n_c) the complexity depends on the length of the list, the list has $n_c!$ inputs, meaning the complexity is $c = \log_2 n_c!$ bits.

- Head times: the head times are discretized in steps of 10 seconds, with a maximum of 60 s. meaning there are six options, this results in three bits per cyclist. If multiple routines are used, the amount needs to be multiplied by the number of routines n_r , hence: $c = 3 \cdot n_c$ bits.
- dropping distance: The dropping distance can be defined in parts of a fifteenth of the total course length. Therefore the complexity is four bits per cyclists: $c = n_c \cdot 4$ bits.

The maximum number of generations was set to 200, however during the convergence tests, this was never exceeded. The rest of the parameters was set to the default settings of MATLAB's built in genetic algorithm optimisation.

3.3. Convergence

It is determined that a genetic optimisation will be used to generate the results, however the accuracy of optimisation depends on the problem as well as the parameters of the genetic algorithm. The genetic algorithm is performed with use of the optimisation toolbox in MATLAB. This toolbox has a function for genetic algorithm [13], which is used. Four parameters (three independent) are varied to assess their influence on accuracy and computational costs. The population size is closely related to the computational costs. The population size determines the number of function evaluations per generation. If the population size causes better convergence, the amount of generations required reach a required accuracy is lower. Elite ratio, mutation ratio and crossover ratio influence the convergence, and thereby also the computational costs, but the influence on the computational costs is not as high as that from the population size. Therefore using a low complexity problem the convergence of different combinations of the Elite-, Mutation- and crossover-ratio are compared.

First a case with lower complexity is used to determine the cross-over ratio, mutation ratio and elite ratio of the genetic algorithm in a strategy optimisation of low complexity. This test simulated a group of four cyclists over a race of five kilometres. A second test, with higher complexity was used to determine the population size, for the best convergence. This test was with eight cyclists over a race of kilometres.

3.3.1. Elite, mutation and crossover ratio

multiple configurations of elite, mutation and crossover ratio are compared using a small complexity problem. The population is split in three categories to produce the next generation, these three categories are elite, mutation and crossover; it is therefore that the sum of the elite-, mutation- and crossover-ratio needs to be 100 %. In this problem from a 5 km team time trial with four cyclists, the order and head times are optimised. This results in 17 bit complexity. For every population size in every test the optimisation is performed 20 times, to provide enough data points. The configurations are based on [20], not all parameters are individually varied to reduce computational costs, the objective is a well converging combination rather than the optimum since the convergence tests will be far more computationally expensive with respect to the actual optimisations. For all configurations the test are performed on population sizes 20, 40, 80, 160, 320 in order to be able to detect their convergence over population size. Later the population size will be selected. The used configurations are presented in table 3.1. in the first three configurations the elite count was set to 5 % and the mutation ratio was varied, test 1 is according to the standard options from MATLAB's genetic algorithm. In [20] it was said that for small population (4, 8) sizes a mutation ratio of 15 % was preferred and for larger population sizes (64, 128) 1 % or 2 % performed better. This lead to the hypothesis that a fixed number of elites and mutations (throughout the population sizes) would perform well, therefore in test 4 the number of elites and the crossover ratio are kept constant and in test 5 the both the number of elites and number of mutated are kept constant.

The results are presented in figure 3.3 in terms of the average velocity. The red line is the value of the maximum velocity of all data sets, the error is defined as the difference of a data point to that value. In this graph it is shown that the two tests with a fixed number of elites (4, 5) did not perform well with respect to the rest, with the largest error with the largest population size. The third test with a low mutation rate took very long to get good convergence, with a large error at a population size of 160. Test 1 and 2 both performed well.

From this little tests it cannot be concluded that a fixed number of elites is not preferred, however given the results presented results it does not seem better. There is no test where the number of mutated is fixed and the number of elite is varied along the population sizes, however the results with the fixed number of elites do not motivate to do so. As test 1 were the standard MATLAB configurations it was no surprise that they performed so well. Test two shows a better convergence with both population sizes 80 and 160, with respect to test 1.

It is chosen to proceed with the configuration from test 2 with an equal elite ratio and a higher mutation ratio and a lower crossover ratio with respect to the MATLAB's standard (test 1). With these settings the tests will be repeated for an optimisation with higher complexity and all considered model configurations.

Table 3.1: The configuration for the small complexity convergence test

Convergence test	Population sizes	Elite count	Mutation count	Crossover ratio
1	20	5 %	15 %	80 %
	40	5 %	15 %	80 %
	80	5 %	15 %	80 %
	160	5 %	15 %	80 %
	320	5 %	15 %	80 %
2	20	5 %	35 %	60 %
	40	5 %	35 %	60 %
	80	5 %	35 %	60 %
	160	5 %	35 %	60 %
	320	5 %	35 %	60 %
3	20	5 %	5 %	90 %
	40	5 %	5 %	90 %
	80	5 %	5 %	90 %
	160	5 %	5 %	90 %
	320	5 %	5 %	90 %
4	20	20 % (=4)	0 % (=0)	80 %
	40	10 % (=4)	10 % (=4)	80 %
	80	5 % (=4)	15 % (=12)	80 %
	160	2.5 % (=4)	17.5 % (=28)	80 %
	320	1.25% (=4)	18.75% (=60)	80 %
5	20	20 % (=4)	10 % (=2)	70 %
	40	10 % (=4)	5 % (=2)	85 %
	80	5 % (=4)	2.5 % (=2)	92.5 %
	160	2.5 % (=4)	1.25 % (=2)	96.25 %
	320	1.25% (=4)	0.625% (=2)	98.125%

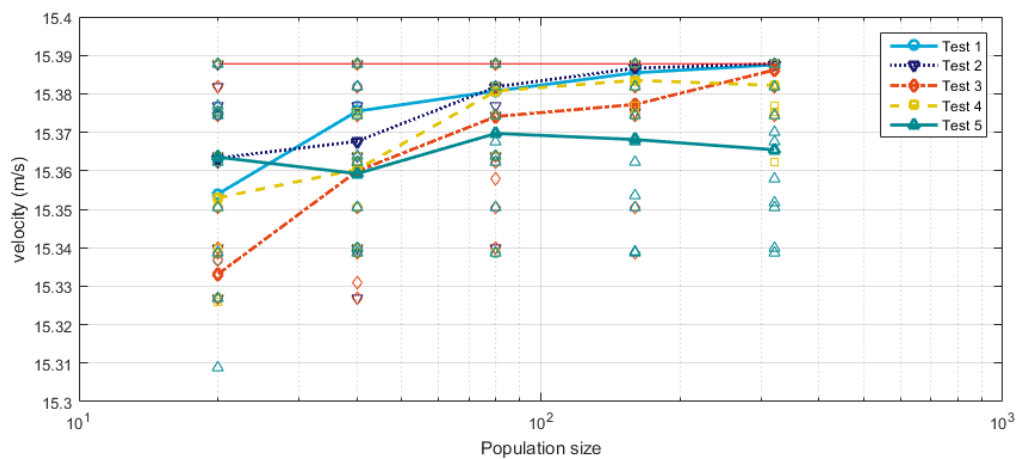


Figure 3.3: Convergence plot of the performed optimisation on the small complexity problem

3.3.2. Population size

With the configurations from the small complexity test, the convergence tests are performed again on a problem of larger complexity, that is the same size as those used later in the study. From these convergence test not only the population for further optimisation is selected, but also the standard deviations are defined, which are used in the statistics of the results. As the standard deviations are expected to be different for the different model configurations, the convergence test is performed for all four model configurations used to obtain the results later. It is therefore also important that an optimisation is performed that results in high standard deviations. The optimisation that is preformed is a order and head times optimisation, with dropping. This results in a 72 bit complexity optimisation. In order to drive the optimisation results to a high standard deviation a very different group was selected, containing two super strong, two strong, two medium and two weak cyclists. In order to obtain a decent amount of head turns the simulation was performed over a 10 km flat road. As with the small complexity test, for each population size 20 optimisations were performed.

The results for the larger complexity test are presented in figure 3.5 and the errors in figure 3.6. From the velocity results it is shown that the means rise towards the estimated maximum velocity, defined as the largest mean velocity found in the data set an plotted as the red horizontal line. Also the standard deviation shrinks with the population size, as is plotted in figure 3.4. It is shown that generally the convergence up to population sizes 80 or 160 is significant and from there it begins to flatten out. Taking in consideration the convergence of both means, standard deviation and the computational costs it is selected to continue with a population size of 160. In cases where more accurate results are required it can be decided to run more optimisations.

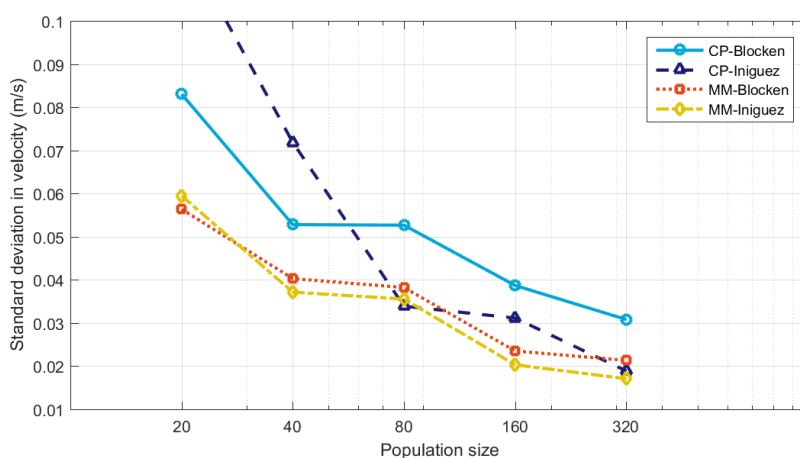


Figure 3.4: The standard deviation on the velocity of the results from the genetic algorithm optimisation against population size.

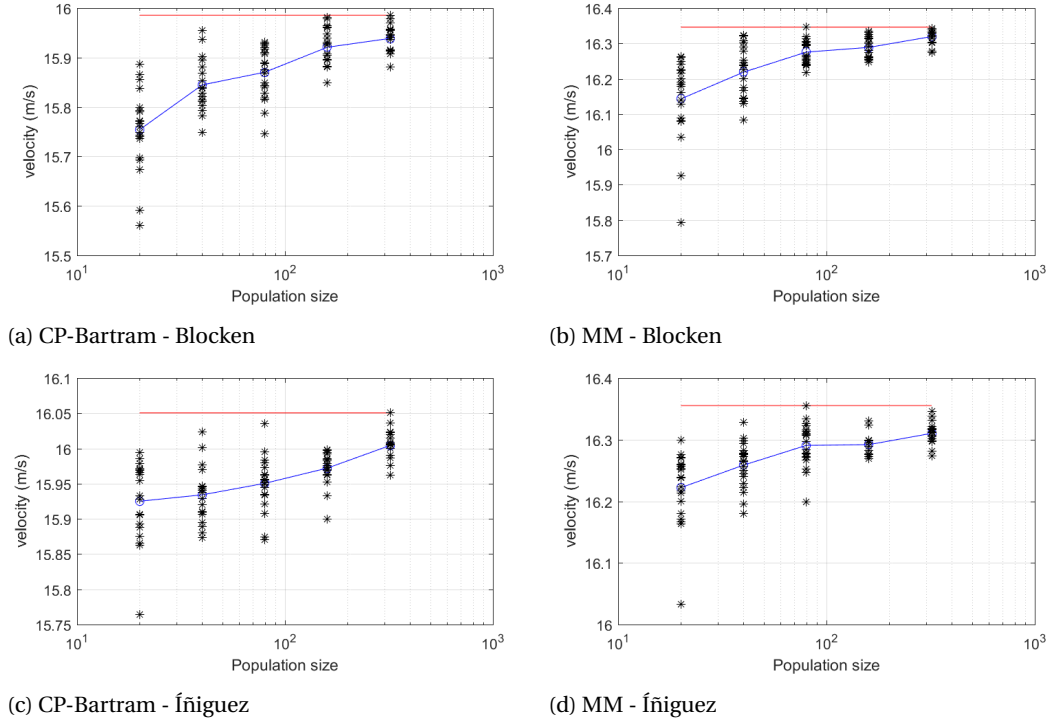


Figure 3.5: Absolute mean race velocity values for the convergence of an optimisation with a 72 bits complexity using a head time optimisation. The same graph is shown for the convergence tests in all four model configurations

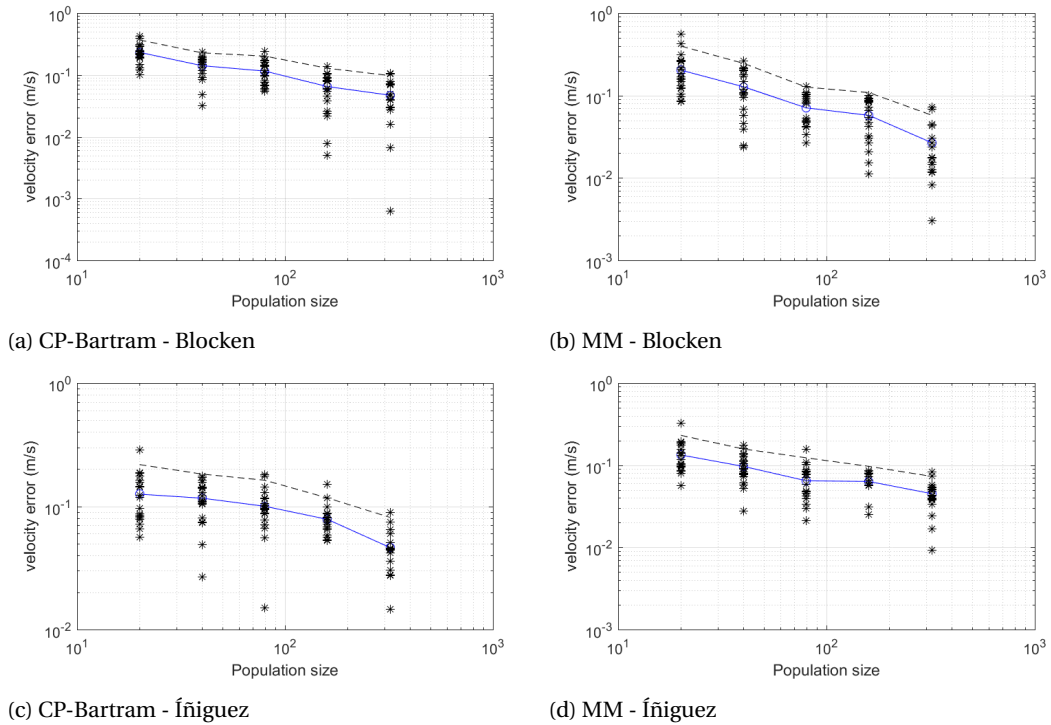


Figure 3.6: Error in mean race velocity values for the convergence of an optimisation with a 72 bits complexity using a head time optimisation. The same graph is shown for the convergence tests in all four model configurations

3.4. Conclusion

In this convergence analysis different parameter combinations have been tested with the genetic algorithm. It is concluded that with the settings, elite ratio = 5 %, mutation ratio = 35 % and cross-over ratio = 60 % a decent convergence is achieved for a head times optimisation problem. The final convergence test with a complexity of 64 bits has shown that the standard deviation drops steep along the tested population sized 20, 40 and 80, and it becomes less steep when passing the population size of 160. The final standard deviations for the model configurations are presented in table 3.2. These standard deviations correspond to a head time optimisation with a considered group of two super strong, two strong, two medium and two weak cyclists. It is assumed that these standard deviations are representative for all head times optimisations with the considered group formation and a complexity equal or lower than 64 bits. Therefore these standard deviations are used in the statistical analysis throughout the study.

Table 3.2: The standard deviations from the convergence tests at a population size of 160 for the four used model configurations.

Model configuration	standard deviation on mean velocity
CP-Blocken	0.0387 m/s
CP-Íñiguez	0.0311 m/s
MM-Blocken	0.0235 m/s
MM-Íñiguez	0.0203 m/s

4

Analysis of a standard team time trial

Before diving into optimising different strategies, an evaluation of a standard strategy team time trial is performed. The analysis will be in three steps, at first the analysis will be made on a team time trial without any balancing. Secondly the performance is improved by performing workload balance by means of adjusting the times spend in first position for different cyclists. In the third case, cyclists are also dropped from the group during the race, to further balance the workload.

4.1. Analysis of the regular strategy without workload balancing

A reference case is presented of a team time trial where a group of cyclists from various strength classes, without any workload balancing measures. The group consist of eight cyclists, where two cyclists from each strength class are considered, meaning: two super strong, two strong, two medium and two weak. All cyclists are from the same weight class, medium. The starting order is in descending strength class, so first the two super strong, then the two strong, then the two medium and at the end the two weak cyclists. The considered race is a flat 30 km time trial, which is completed with a constant velocity of 15.182 m/s. The team uses a standard strategy, where all cyclist do 30 seconds in first position and change from first to last position. The simulation was performed using the CP-model for physiology and Blocken's aerodynamic interaction coefficients. The resulting physiological states are presented in figure 4.1.

The results from the physiological state show that the depletion of the anaerobic capacity is disproportional higher for the weaker cyclists with respect to the others. As presented in figure 4.1 the anaerobic capacity (W'_{Bal}) of the weak cyclists are nearly empty at the end of the race, while all other cyclists still have more than half of their capacity left. The mean power output during the race of all cyclists lays between 376 W and 380 W, meaning that the workload is divided more or less equal among the cyclists, however this is below the critical power for the super strong, strong and medium cyclists, but above the critical power for the weak cyclist.

Table 4.1

cyclist	Head Time	Average power	effective workload
Super strong 1	30 s	382 W	85.1 %
Super strong 2	30 s	383 W	85.1 %
Strong 1	30 s	382 W	90.9 %
Strong 2	30 s	381 W	90.6 %
Medium 1	30 s	380 W	97.5 %
Medium 2	30 s	380 W	87.4 %
Weak 1	30 s	380 W	105.5 %
Weak 2	30 s	380 W	105.5 %

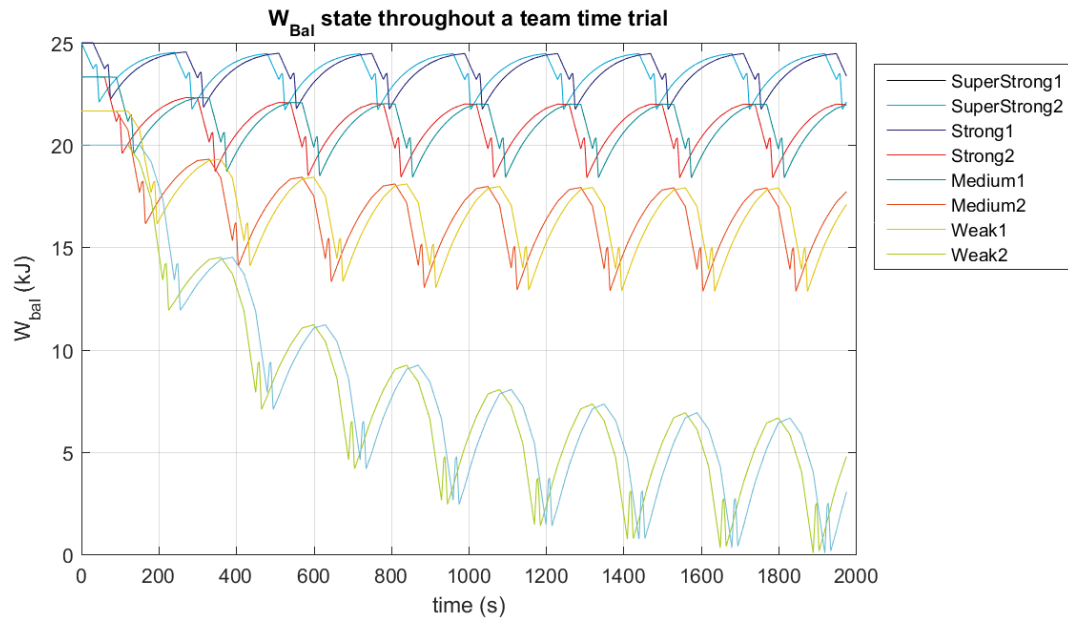


Figure 4.1: An example of the W_{Bal}^I states of cyclists during a team time trial. The top two lines represent the super strong cyclist, the two lines below that, the strong cyclists, followed by two medium cyclists, and the bottom lines represent two weak cyclists. The head times of the cyclists are equal with 30 s in this example.

4.2. Head time optimisation

A workload balancing is attempted by adjusting the head times corresponding to the strength class of the cyclists. The head times were optimised with the genetic algorithm, with population size of 160, only one optimisation was performed. The physiological states are much closer together throughout the race. The velocity was raised with 0.207 m/s from no workload balance to 15.389 m/s with head times balancing. The resulting physiological states are presented in figure 4.2. In this graph is shown that it is still the weak cyclist that limit the group performance. It is therefore suggested that dropping these two cyclists somewhere during the race will allow them to perform their contribution to the overall performance, while not having to complete the entire course.

4.3. Head time optimisation with dropping

With dropping the result in terms of velocity is raised with 0.223 m/s from head times optimisation to 15.613 m/s. Therefore the dropping can be considered as important as the head times balancing. The physiological states are presented in figure 4.3. Because both the weak and the medium cyclists are dropped during the race a higher velocity could be achieved. It can be seen that while the group is still with eight or six cyclists the physiological states of the strong and super strong cyclists remain high, however when the group size drops to four the anaerobic reserve is depleted rapidly. This is of course because both the mean drag over the positions rises and the cyclists will visit the high drag first position more frequent.

4.4. Discussion

As a result of the efforts to reduce the time the weakest cyclists spend in first position and increase the time the stronger cyclists spend in first position it is shown in figure 4.4 that the workload is more balanced with the head time optimisation and even more balanced if also dropping is considered. In this graph on the horizontal axis the cyclists are presented, each having a bar corresponding to the cases of no balancing, head times balancing and head times balancing with dropping. On the vertical axis the relative workload is given as a percentage. The relative workload is given by the mean power divided by the critical power. When a cyclist is dropped the power until the drop point is considered. The work demands using the different strategies are not exactly equal. Still the strategies use workload balancing to increase their performance therefore the strategy performs as expected if the workload is balanced correctly. It is shown that the balancing with head times is better than with no balancing. And that with head times optimised an dropping considered

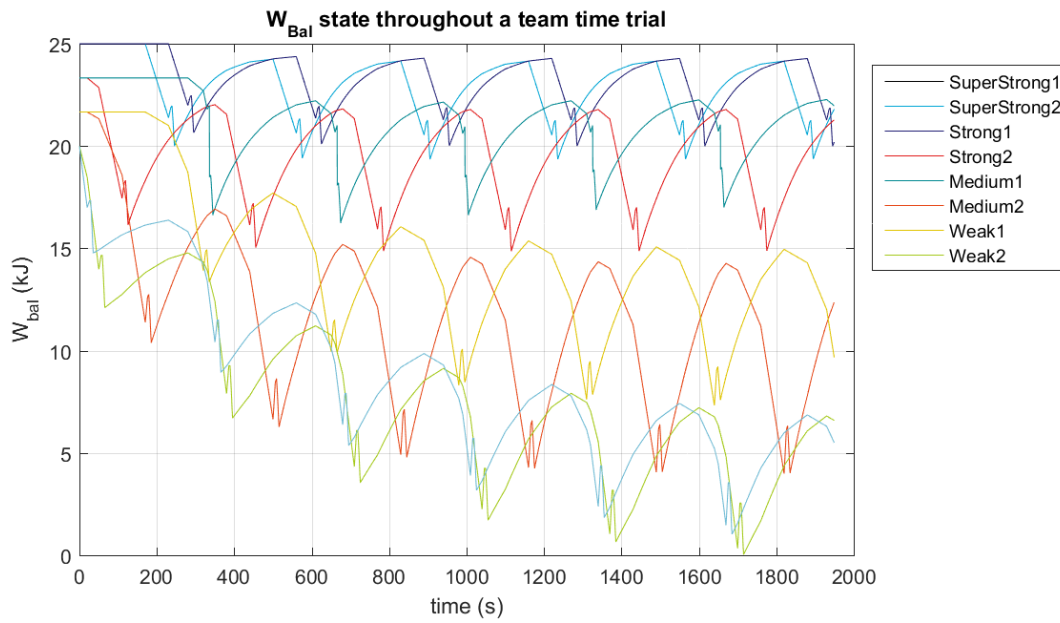


Figure 4.2: An example of the W'_{Bal} states of cyclists during a team time trial. The physiological states alternate through each other and are therefore slightly difficult to distinguish, however from top to bottom the states of two super strong, two strong, two medium and two weak cyclists are displayed. The head times are 10 s for weak, 20 s for medium, 30 s for strong and 40 s for super strong cyclists.

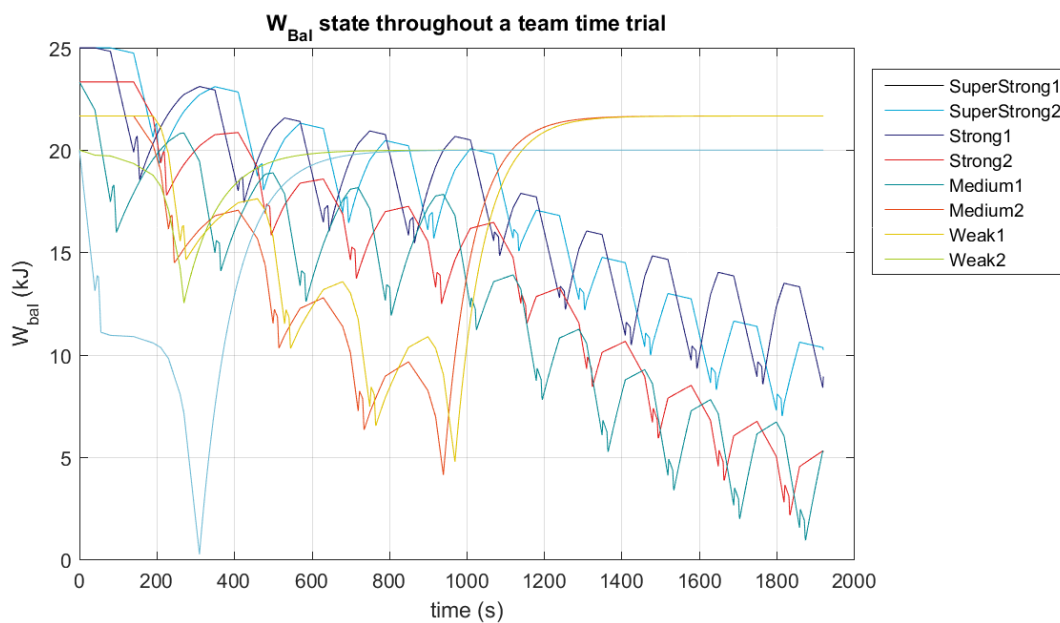


Figure 4.3: An example of the W'_{Bal} states of cyclists during a team time trial. The physiological states alternate through each other and are therefore slightly difficult to distinguish, however from top to bottom the states of two super strong, two strong, two medium and two weak cyclists are displayed. The head times are 10 s for weak, 20 s for medium, 30 s for strong and 40 s for super strong cyclists.

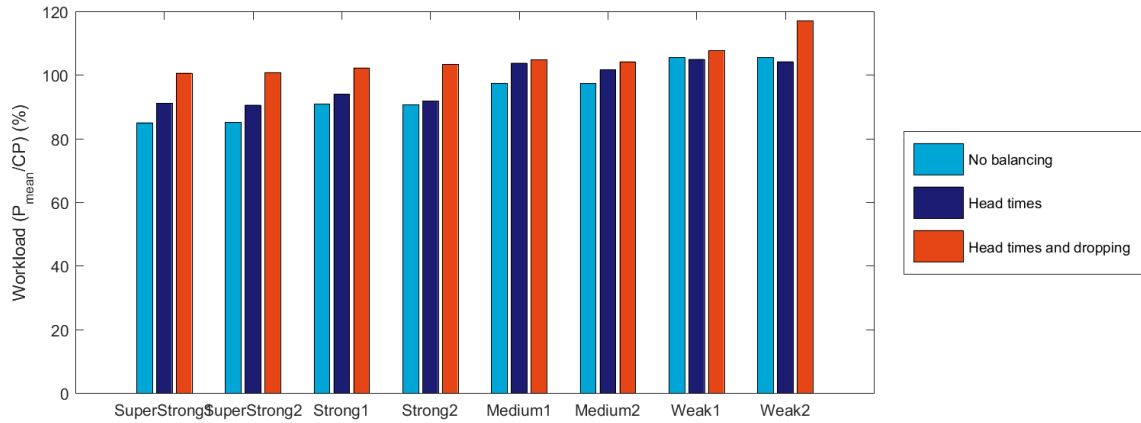


Figure 4.4

the strategy is much more balanced than the others. Even so with all strategies the weak cyclists perform relatively more workload than the other cyclists.

4.5. Conclusion

The workload balancing strategies evaluated in this chapter have shown that head times balancing improves the workload distribution and the performance. Head times optimisation with dropping improves workload distribution even more and also the performance is better, considering this group of cyclists. Even with head time balancing and dropping it could not be avoided that the weaker cyclists take up more relative workload. During the following chapters strategies will be evaluated that attempt to distribute the workload even further.

5

Order optimisation

Four orders have been suggested for different reason, these orders are compared by applying a head time optimisation and assessing their performance. The selected orders will be tested on a flat road of 30 km. The group is composed of eight cyclists, of which every physiological strength group is represented by two cyclists, resulting in two super strong, two strong, two medium and two weak cyclist. The simulations are performed with all cyclists of weight class medium. Since there is no incline in the course this is present. During the team time trial dropping cyclists is included in the strategy and the time of the fourth cyclist counts. To asses an order a head time optimisation is applied, to optimise the workload among the cyclists. The optimisations are performed for four model configurations: CP Bartram - Blocken, CP Bartram - Íñiguez, MM - Blocken, MM - Íñiguez. The orders which are selected come from different perspectives and are presented in table 5.1. The reasoning why the orders are selected is discussed in the following paragraph.

Order 1 The first order has each cyclist of a different strength class be followed by one that is equal or weaker than itself, apart from the last where a weak cyclists is followed by the super strong cyclist that started in first position. When considering Blocken's aerodynamic interaction model, the cyclists in second and third position will have an increased drag from the cyclists further downstream. This makes that the head times of the two cyclists in front will effect the workload of the considered cyclist. This is far less the case when considering Íñiguez's aerodynamic interaction model. And the strength class jump from super strong to weak makes that the two super strong cyclists should not have too long head times, to reduce workload on the weak cyclists.

Order 2 The second order is selected because in contrast to the first order it, the cyclists will be negatively affected by the drag increase in second and third position in Blocken's aerodynamic interaction model. Under the assumption that the optimisation will pick large head times for stronger cyclists, the result will be that over the high head times will be more spread, making the cyclists have more equal recovery times, therefore not more for the weaker cyclists. This order was suggested because of practical advantages rather than theoretical advantages, because of the spread of the physiological capacity, the frequency of changing will be more

Table 5.1: The orders considered in the order analysis

Order no	Pos. 1	Pos. 2	Pos. 3	Pos. 4	Pos. 5	Pos. 6	Pos. 7	Pos. 8
1	Super Strong	Super Strong	Strong	Strong	Medium	Medium	Weak	Weak
2	Super Strong	Weak	Super Strong	Weak	Strong	Medium	Strong	Medium
3	Super Strong	Medium	Strong	Weak	Super Strong	Medium	Strong	Weak
4	Super Strong	Strong	Medium	Weak	Weak	Medium	Strong	Super Strong

constant, theoretically this does not change much, however in reality this is expected to improve structure in the group.

Order 3 The third order is quite similar to the second, however in this case the strength level differences are reduced, such that there is a minimum of one and a maximum of two levels. This way the physiological capability is spread over the group, while reducing the strength difference with respect to order 2.

Order 4 The fourth order is focussed on having the lowest performance difference among the following cyclists. This done because than a cyclist will be in second position when a cyclists of similar performance is in first, meaning that a large amount of time spend in first position results a large amount of time spent in second position by a cyclist of similar performance.

Hypothesis It is expected that while using Blocken's aerodynamic interaction model, the orders that allow for the largest workload differences will result in the best scores. This will be the order 4 as best. It is expected that letting the super strong cyclists be followed by the weak cyclists, the contribution of the super strong cyclists to the group performance will be reduced. Therefore it is expected that with Blocken's aerodynamic interaction model order 1 will perform worse with respect order 4 and significantly better than order 2 and order 3. It is also expected that with Blocken's aerodynamic interaction model order 3 will perform better than order two. Since the workload distribution with Íñiguez's aerodynamic interaction model the workload distribution is much less effected by the order that the there will be no significant differences among the orders.

Table 5.2: Results in form of the average velocity of the group during the 30 km team time trial with different orders, with dropping (n = 5 for all optimisations)

Order no	Result CP, Blocken	Result CP, Íñiguez	Result Blocken	MM, Íñiguez	MM, Blocken
1	15.428 m/s	15.897 m/s	15.440 m/s	15.772 m/s	
2	15.291 m/s	15.864 m/s	15.354 m/s	15.752 m/s	
3	15.327 m/s	15.823 m/s	15.335 m/s	15.704 m/s	
4	15.519 m/s	15.902 m/s	15.460 m/s	15.798 m/s	

Table 5.3: Significance of the hypotheses over the different models

Hypothesis	Result CP, Blocken	Result CP, Íñiguez	Result Blocken	MM, Íñiguez	MM, Blocken
Order 4 > Order 1	Confirmed ($P = 0.0001$)	Not significant ($P = 0.3981$)	Not significant ($P = 0.0866$)	Confirmed ($P = 0.0227$)	
Order 3 > Order 2	Not significant ($P = 0.2621$)	Confirmed ($P = 0.0185$)	Not significant ($P = 0.1002$)	Confirmed ($P = 0.0001$)	
Order 1 > Order 2	Confirmed ($P = 0.0000$)	Confirmed ($P = 0.0453$)	Confirmed ($P = 0.0000$)	No ($P = 0.0563$)	
Order 1 > Order 3	Confirmed ($P = 0.0000$)	Confirmed ($P = 0.0001$)	Confirmed ($P = 0.0000$)	Confirmed ($p = 0.0000$)	

5.1. Results

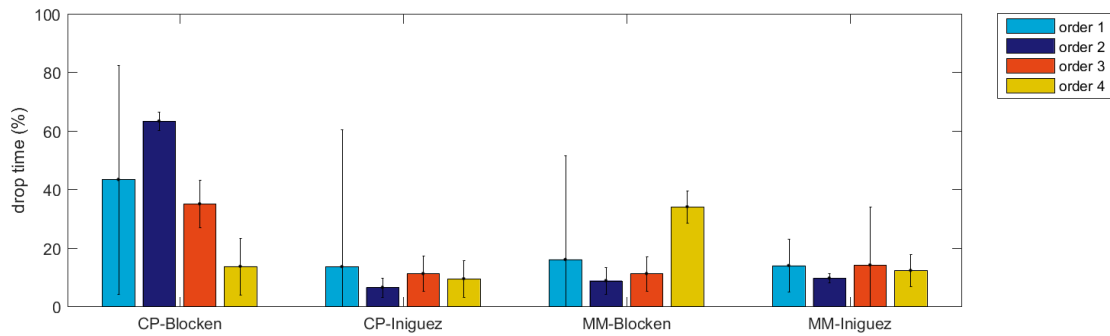
The results of the optimisations for the order are presented in terms of their mean velocity. The velocities corresponding to different orders are presented in table 5.2, these are the means of all five optimisations. The results are considered significant if $p < 0.05$.

The mean values correspond to nearly all hypotheses, only the mean velocity of order 2 is lower than that of order 3 in stead of larger, while using the CP-Blocken model configuration. In all other cases the results are as expected, however not all of the hypothesis can be confirmed with significance, weather or not the hypotheses are confirmed is presented in table 5.3. The first hypothesis that order 4 is better than order 1 is confirmed by two model configurations (CP-Blocken and MM-Íñiguez), as expected the differences are not large (0-0.030 m/s) except for the CP-Blocken configuration where the difference is 0.091 m/s. The second hypothesis that order 3 is better than order 2 is confirmed by two model configurations (CP-Íñiguez and MM-Íñiguez). In the CP-Blocken configuration it was found that order 2 performs better than order 3, but without statistical significance. The third hypothesis is, that order 1 is better than order 2 is confirmed by three out of the four model configuration, only the model configuration MM-Íñiguez did not confirm this. The last hypothesis that order 1 is better than order 3 is confirmed by all model configurations.

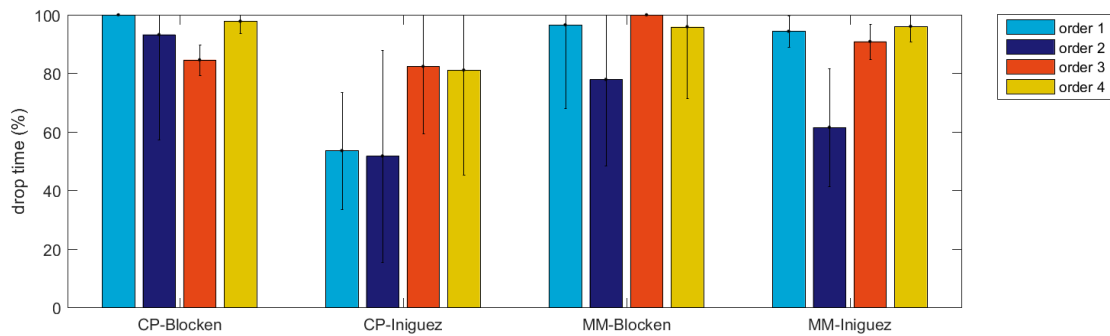
5.2. Discussion

When observing the results in table 5.2 it becomes clear that the differences in the CP-Blocken model configuration are largest, with a maximum difference of 0.228 m/s. The smallest difference in all other model configurations are considerably lower (0.079 m/s for CP-Íñiguez, 0.096 m/s for MM-Blocken, 0.094 m/s for MM-Íñiguez). That the differences when using Íñiguez's aerodynamic interaction model are slower is expected, however it was expected that the differences in when using the MM-Blocken configuration would be larger. In B it is demonstrated that both model react different to different types of intermittent exercise. It could well be that the differences in physiological reaction to the different power profiles, introduced by the strategy in combination with Blocken's aerodynamic interaction model, is less with the MM-model than with the CP-model.

Even though the difference in drafting coefficients in second, third and fourth positions have such little differences in Íñiguez's aerodynamic interaction model, there are still clear benefits of the workload balancing techniques in orders 1 and 4. With Íñiguez's aerodynamic interaction model the highest drag beside the first position was found in the last position instead of the second position, when a cyclist spends a long time in



(a) Drop times for the weak cyclists for the results of the simulations of all four orders using all four model configurations



(b) Drop times for the medium cyclists for the results of the simulations of all four orders using all four model configurations

Figure 5.1: Relative drop times ($t_{\text{drop}}/t_{\text{finish}}$) of the weak and medium cyclists over all optimisations, catagorised by order and model configuration. «maybe adjust y labels, drop time is not ideal»

first position, it is not the cyclist behind, but the cyclist in front (who is now in last position) that is affected. With the considered orders there is no order that benefits from this effect, it also has to be considered that the drag increase in the last position with respect to the one-but-last position is also present in Blockens aerodynamic interaction model only with less difference.

It is expected that if workload balancing is successful, the cyclists of weak and medium strength class are dropped out of the group late. Figure 5.1 shows the drop times, for the medium and weak cyclists. A drop time of 10 % means that the cyclist is dropped at 10 % of the finish time, a drop time of 100 % means that the race is completed and effectively the cyclist is not dropped. In figure 5.1a the drop times for the weak cyclist is shown, the results here seem to be more model dependent than order dependent. It is shown that the weak cyclist are in most occasions dropped very soon (before 20 %). It is presented in figure 5.1b that the cyclists of medium strength are dropped later. It is clear that in the best performing orders (1 and 4), but also order 3, the medium strength class cyclists are kept with the group longer than order number 2.

Since the weaker cyclists are dropped very soon (often before 20 %), the orders that remain after this event are also important to assess. The orders remaining after the dropping of the two weak cyclists are presented in table 5.4, with order 1 and 4, which have low differences between cyclists strength class of following cyclists, there is still little difference after dropping. With order 2, the difference between strength classes of following cyclists is reduced a lot, now the two super strong cyclists are placed after each other, followed by altering medium and strong cyclists. With order 3 still has a lot of differences in following strength classes.

It must be noted that in this study the aerodynamic drag area ($C_d A$) is equal for all cyclists, therefore a cyclist of a higher strength class is also has a better performance. In situations where cyclists are of different sizes and weights it is not the strength class but the critical velocity (CV) that determines it's performance. However it must also be noted that cyclists of different shapes and sizes, also have different aerodynamic

Table 5.4: The orders that remain after dropping the weaker cyclists

Order no	Pos. 1	Pos. 2	Pos. 3	Pos. 4	Pos. 5	Pos. 6
1	Super Strong	Super Strong	Strong	Strong	Medium	Medium
2	Super Strong	Super Strong	Strong	Medium	Strong	Medium
3	Super Strong	Medium	Strong	Super Strong	Medium	Strong
4	Super Strong	Strong	Medium	Medium	Strong	Super Strong

interactions. For example Heimans et al. (2017) [22] has shown that when a larger cyclists following a smaller cyclist results in a larger drag reduction for the following cyclist, than when the cyclists switch their positions.

5.3. Conclusion

It has been shown that when balancing workload over groups of cyclists, with a large variety in performance, using only head times to balance the workload; the starting order is of great importance to performance. Depending on the model that is used to assess the performance the performance difference ranges between 0.079 m/s and 0.228 m/s in average velocity or 9.42 s to 28.8 s in finish time over a 30 km flat team time trial. It was found that having less performance differences between the cyclists following each other resulted in the best performing orders. The best performing order had a maximum of 1 level difference in strength classes following each other. Orders where stronger and weaker cyclists were altered performed significantly less than orders that minimised the performance differences between following cyclists. Aerodynamic differences among cyclists were not considered, but are expected to have influences on the results, also this data is for a flat team time trial, if there would be a climb in the race, the effect of differences in mass are also expected to influence the results.

6

Adjusted Return Positions Strategy

The workload balancing is performed by adjusting the ratio between time spend in different positions. With the standard strategy, the amount of times a cyclists is in a specific position is equal over the cyclists, considering that no cyclists is dropped. The times are balanced by adjusting the time of the cyclist in first position. It is shown in chapter 4 that without dropping, this does not create enough balance in the presented group (2 x super strong, 2 x strong, 2 x medium and 2 x weak). It is shown that the balancing error is reduced severely by dropping weaker cyclists, however by doing so this increases the mean drag among cyclists and therefore requiring more power to reach the same velocity. In this chapter a workload balancing method will be presented that adjust the frequency that a cyclists is in different positions.

Instead of adjusting the amount of time spend in a position during a race by adjusting the duration of each time the cyclist reaches that position; the amount of time can also be adjusted by changing the amount of times a cyclist reaches that position. This strategy aims to do this by letting the cyclists change from first position not only to last but any position. Each cyclist will have its own position to return to. An example of a group of four cyclists is shown in figure 6.1. This means that the order is changing as the cyclists change position. Also depending on the start order the changing with different return positions may turn out in a different pattern. The aim is that by letting stronger cyclists return to positions in front of the last, the weaker will get more time to recover from their workload contribution in the front positions. A difference between the two aerodynamic interaction models is expected to be large and will be discussed in the next paragraph.

Using this strategy it is important to know which positions a cyclist recovers and which positions it expends. The border between these physiological phases is described by the critical velocity. This critical velocity represents the velocity above which anaerobic energy is expended and above which anaerobic energy is recovered, this is defined per position per cyclist. For both aerodynamic interaction models and different cyclists this is visualised in figure 6.2, the two graphs represent the two aerodynamic studies. On the horizontal axis the positions are noted, at each position there is a bar reaching to a critical velocity that belongs to the cyclist type as is noted in the legend. As a short recap it is noted that if the velocity exceeds the critical velocity the cyclist will not recover in this position. For both Blocken's and Íñiguez's models the highest critical velocity for the weak cyclist is about 15.5 m/s (Blocken: 15.60 m/s, Íñiguez: 15.45 m/s). As this corresponds to the maximum value found in the order optimisation, it is expected that the weak cyclist will not recover at all. Even so the medium cyclists peak at around 16 m/s (Blocken: 16.05 m/s, Íñiguez: 15.895 m/s) Therefore also they will need a lot of recovery time.

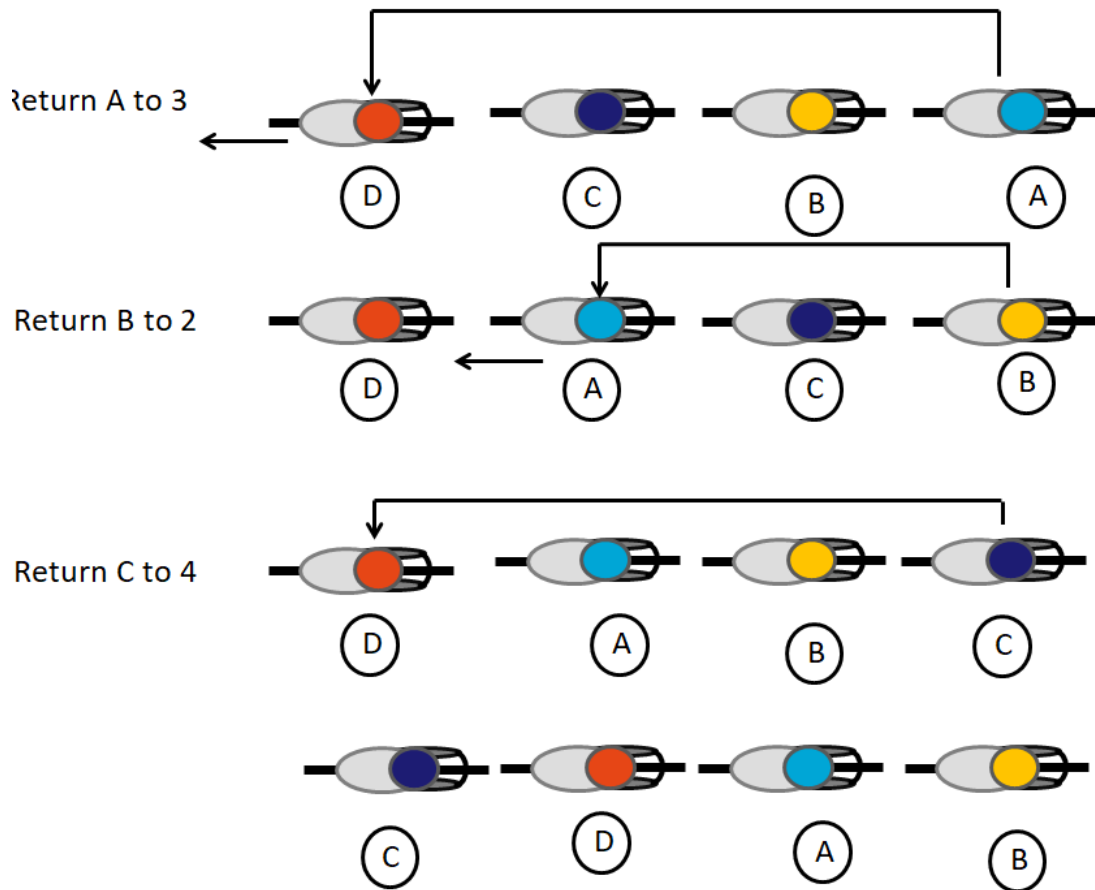
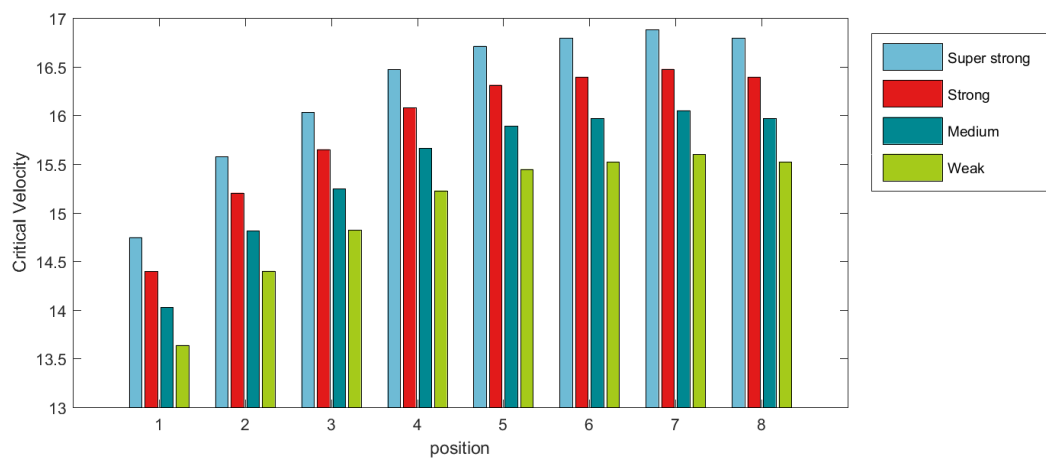
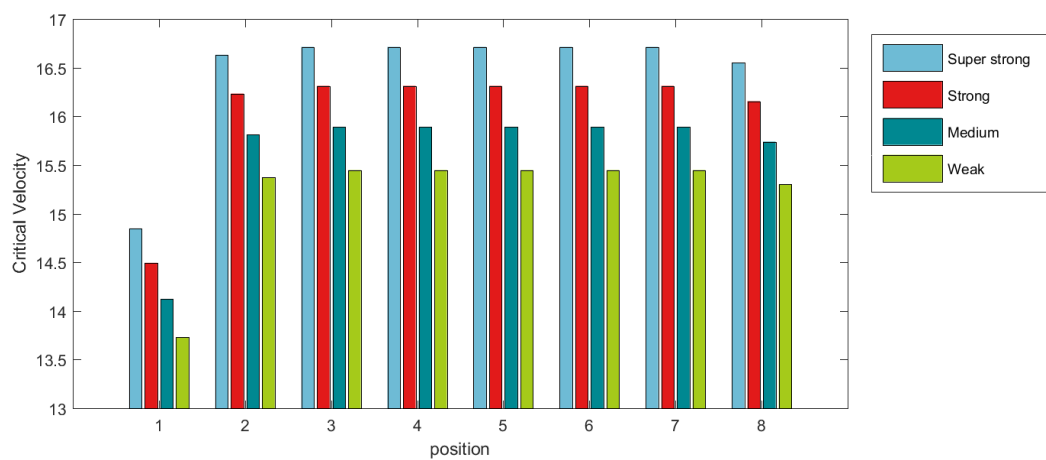


Figure 6.1: An example of changing with the return positions strategy. In this example A changes to 3, B changes to 2 and C changes to 4.



(a) Blocken



(b) Íñiguez

Figure 6.2: Critical velocities in different positions, using the CP model combined with Blocken's aerodynamic interaction model (a) and Íñiguez's aerodynamic interaction model (b)

6.1. Selected return positions

It was tried to optimise the return positions using the genetic algorithm, however the convergence turned out poor, by trying different options manually a better result could be obtained very easily. It is expected that the poor convergence of the optimisation is a result of the effect that by adjusting the return position of one cyclist, the result could be that some of the cyclists do not get up front any more.

Instead of optimisation some configurations of return positions were tested. Starting with order 1 from chapter 5, different orders were tried, however using most configuration the order changed to the same order after a few changing routines. This was tested by performing simulations with the CP-Blocken model configuration, head times were set to 30 s for each cyclist on a 30 km flat course. The configuration started by having all cyclists with return position 8 and then decreasing those of the cyclists that were the least depleted at the end of the race. This resulted in the stronger cyclists returning to lower positions and weaker cyclists to later positions. The configuration is presented in table 6.1, including initial positions and the return positions. As explained in the previous section, the weak cyclists are not expected to have any recovery time, therefore the medium cyclist return to position 6, leaving the two weak cyclists in the last positions. This way they do not contribute a lot to the group however they do cause the drafting coefficients in positions 5, 6 and 7 to be lower and thereby contribute to the group performance.

Table 6.1: The initial positions and return positions for the two selected configurations

Cyclist	initial position	Return positions
Super strong 1	1	4
Super strong 2	2	4
Strong 1	3	5
Strong 2	4	5
Medium 1	5	6
Medium 2	6	6
Weak 1	7	8
Weak 2	8	8

6.1.1. hypotheses

It is expected that using this strategy, large differences in individual performance are balanced better. Since this group composition has large individual differences, it is expected that this strategy performs better than the head time balancing for the tested order. It is also expected that there will be a small difference between the head times optimisations and the fixed head times cases in the advantage of the head time optimisation.

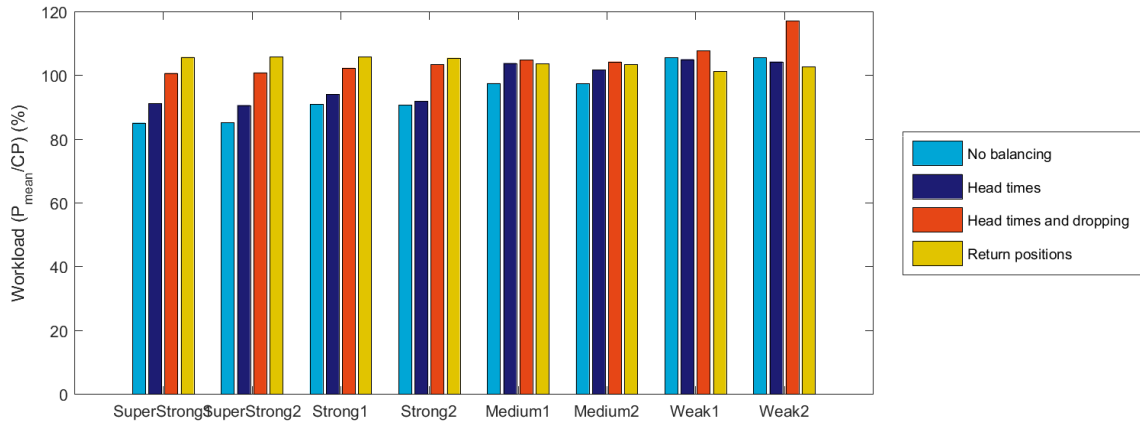
Since with Blocken's aerodynamic interaction model has a reduced drafting and therefore higher drag in positions 2, 3 and 4 with respect to Íñiguez's model, it is expected that with Íñiguez's model there will be less difference between the velocities found in the order optimisation and the return positions optimisation. Regarding the fixed head times versus optimised head times in the return positions analysis about the same difference is expected for both aerodynamic models.

6.2. Results

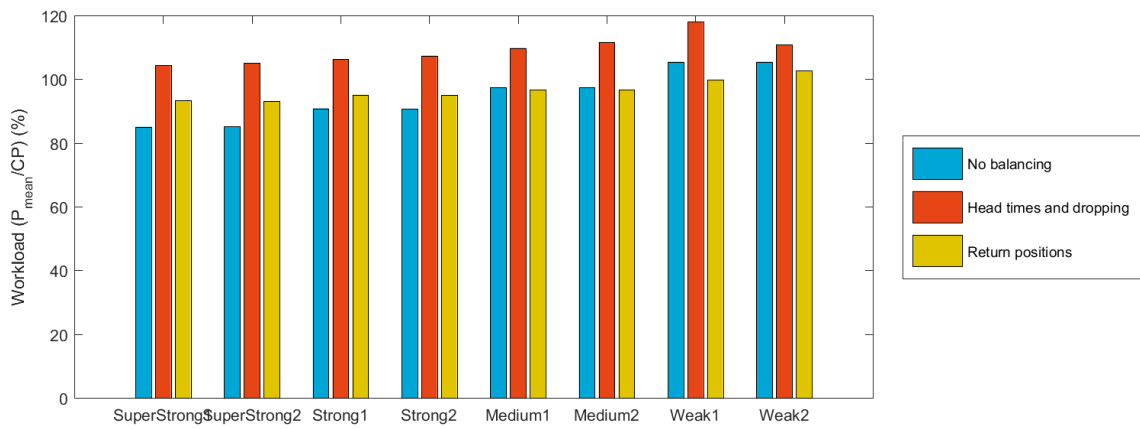
The outcomes of the simulation show some mixed results for this strategy. The results are presented in table 6.2. It can be found that for Blocken's aerodynamic model, the adjusted return positions result in a higher velocity with respect to the head times optimisation. With Íñiguez's model the results are exactly opposite. In this case the statistical relevance is very high ($p < 0.0001$).

Table 6.2

Strategy	Result Blocken	CP, Íñiguez	Result Íñiguez	CP, Blocken	Result Blocken	MM, Íñiguez	Result Íñiguez	MM, Blocken
adjusted return positions	15.786 m/s		15.554 m/s		15.679 m/s		15.667 m/s	
Head times (with dropping)	15.428 m/s		15.897 m/s		15.440 m/s		15.772 m/s	



(a) Blocken



(b) Iniguez

Figure 6.3: The workload balance graph including the balancing strategies: no balancing, head times balancing, head times balancing with dropping and adjusted return positions, all corresponding to the optimisations performed using the CP physiological model

6.3. Discussion

Considering the mean velocities in these results with respect to the critical velocities it is shown that in case of the Íñiguez aerodynamic model the velocities get so high that the weaker cyclists need to be dropped in order to achieve a higher velocity. The concept of this strategy is to let the weaker cyclists make a contribution to the group performance. This is not achieved with Íñiguez's model, however it is likely that in a different group composition this strategy will have also have a positive effect. It is also because the tested configuration was optimised on Blocken's model that it is more likely to be not the best performing configuration considering Íñiguez's model.

In figure 7.1 it is presented that the workload is best distributed with Blocken's aerodynamic model using the return positions adjustment strategy, this is because in this case the mean power to critical power ratio is high and about equal over all cyclists. When considering Íñiguez's aerodynamic model the same strategy is about as well distributed as no balancing strategy at all. This implies that the low velocities in the results with this aerodynamic model are indeed because the workload is not well balanced.

Considering Blocken's aerodynamic model a remarkable increase in velocity is achieved, with 0.358 m/s for the CP physiological model and 0.239 m/s for the MM physiological model. It is shown in figure 7.1 that the workload balancing worked at least using the CP physiological model. This figure shows the relative performance a cyclist was able to deliver, it is shown in this figure that from the head times optimisation with dropping, the stronger cyclist (strong and super strong) have now a higher relative workload with respect to the weaker cyclists (medium and weak). Ideally this would be exactly equal for all cyclists it is expected that if the head times would be optimised for this strategy the workload would be even more spread.

6.4. Conclusion

The concept of balancing workload through the adjustment of return positions has proven to have potential. With Blocken's aerodynamic model depending on the considered physiological model an improvement of 0.358 m/s (CP) or 0.239 m/s (MM) is made. Using the considered group of cyclists and configuration no improvement was found by using Íñiguez's aerodynamic model. In this study it is only demonstrated that this method of balancing has potential, but further study is required to define the properties of a case in which this workload balancing technique can be advantageous. It must also be noted that this strategy shows that the aerodynamic interaction model has a large influence on the effectiveness of the workload balancing strategy.

7

Skipping Strategy

When using the different return positions strategy might seem interesting in theory it is expected to be hard to execute. Not only does the changing cyclist need to know where to re-enter the group, but also the cyclist, which is behind that position needs to leave a gap. In chapters chapter 4, chapter 5 and chapter 6 is explained that a large part of the success in the strategy is determined by the ability of a strategy, to decrease the workload on the weakest cyclists in the group. This has led to a new concept of changing, which is based on the strategy with different return positions, however has a lower level of complexity in execution.

The new proposed strategy is version of the different return positions strategy where the return positions are limited. With this strategy the two weakest cyclists in the group need to be determined. These cyclists will be altering in changing along with the rest and occupying the last position. The way this works it that all cyclists return to the 7th (out of 8) position except the two weakest, they always move to the tail of the group (8th position). This way the two weakest cyclists will always leave a gap for the returning cyclist, except when the other returning cyclist is also a weaker cyclist. The effect is that the two weakest cyclists will spend half of the time in positions 1-7 with respect to the others. The finer workload balancing will be performed by head times adjustments. The optimisations on this strategy will be performed with yet again the same group of cyclists with two of each strength class. This will be easy to compare the results.

7.1. hypothesis

It is expected that with skipping and head times optimised, there will be more opportunity to balance the workload between the stronger and the weaker cyclist. For this reason it is expected that skipping and head times optimisation increases performance with respect to the head times optimised without skipping. It is also expected that with the adjusted return positions and no head times optimisation, there will be even more opportunity to balance workload among cyclist. Therefore it is expected that skipping and head times optimised will not outperform the adjusted head times strategy. It is also expected that there will be a difference in improvements between studies performed with Blocken's aerodynamic model with respect to Íñiguez's aerodynamic model. Since this strategy is partially based on the return positions adjustment strategy, which did not improve the performance when using Íñiguez's model. Also head time balancing is less problematic with Íñiguez's model it is expected that the improvements with this strategy are less present or it does not perform better at all.

7.2. Results

The results of this optimisations show some remarkable results. The results are presented in table 7.1 here the mean velocities over the race are displayed for the four model configurations. Also given are the results for the head times optimisation of this order (also found in chapter 5) and the adjusted return positions, without head times optimised. The optimisation was performed twice and the results that are displayed are the means of these optimisations. The significance is presented in table ??.

Table 7.1: The results in terms of mean velocity of the head times optimisation regarding using the skipping strategy (top row). The results are compared to the results of the head times optimisation of the same order without skipping (= order 1 from order optimisation) and the Adjusted return positions.

Configuration	CP-Blocken	CP-Íñiguez	MM-Blocken	MM-Íñiguez
Head times optimised with skipping (n = 7)	15.628 m/s	16.069 m/s	15.549 m/s	15.975 m/s
Head times optimised without skipping (n = 5)	15.428 m/s	15.897 m/s	15.440 m/s	15.772 m/s
Adjusted return positions (n = 1)	15.786 m/s	15.554 m/s	15.679 m/s	15.667 m/s

Table 7.2: The significance corresponding to the results and hypotheses for the skipping strategy

Configuration	CP-Blocken	CP-Íñiguez	MM-Blocken	MM-Íñiguez
Head times optimised with skipping performs better than without skipping	Confirmed ($P = 0.0000$)			
Head times optimised with skipping performs better than the adjusted return positions	Denied ($P = 0.0001$)	Confirmed ($P = 0.0000$)	Denied ($P = 0.0000$)	Confirmed ($P = 0.0000$)

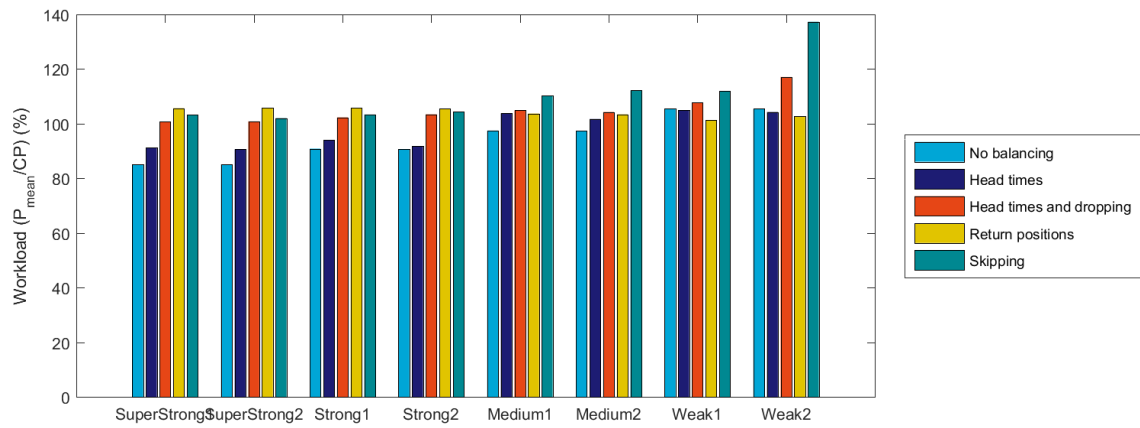
7.3. Discussion

It is surprising that with this strategy the results with Íñiguez's aerodynamic interaction model perform better than the in the head times optimisation, since with the adjusted return positions all results simulated with Íñiguez's model performed worse. However when the results are further analysed it was found that in both optimisation performed with the CP-Íñiguez model it was found that the two weakest cyclists were dropped before the first 25 % of the race. However this does mean that the contribution of the two weak cyclists within this first section was effective enough to improve the result from the head times optimisation. With Blocken's aerodynamic model the results of the skipping strategy perform better than in the head time optimisation and worse with respect to the adjusted return positions optimisation, just as expected.

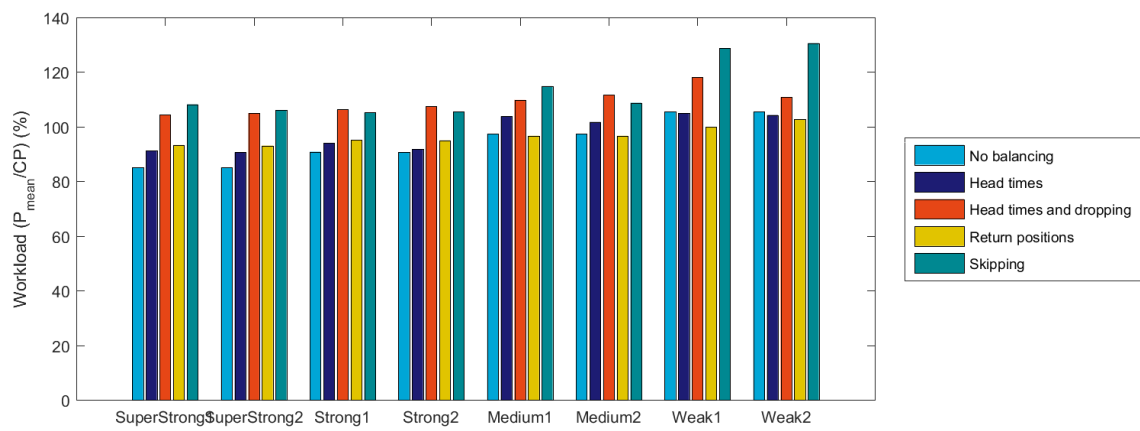
When considering the workload distribution graphs as presented in figure 7.1 the first thing that might surprise is the high relative workload of the weak and medium cyclists, this is explained by the fact that because they are dropped soon in the race they deplete their anaerobic work capacity in a shorter time and are therefore able to produce a higher power according to the critical power theory [30]. Considering the graph corresponding to Íñiguez's aerodynamic model the relative workload for both skipping is about equal to that of head times with dropping and does therefore provide no explanation to why the skipping strategy works better than the head times balancing with dropping strategy. When observing the graph corresponding to Blocken's aerodynamic interaction model the strongest four cyclists have a lower relative workload with respect to those of the adjusted return positions, which does explain why it is not performing better, however just as with Íñiguez's aerodynamic model the relative workload results of the four strongest cyclists with the skipping strategy are more or less equal to those with the head times balancing strategy.

7.4. Conclusion

This strategy provides an attempt at better workload distribution while being less complex to execute with respect to the adjusted return positions strategy. The results show that it causes an increment of 0.088 m/s to 0.210 m/s with respect to the head times balancing, depending on the model configuration. Because the results show that the weaker cyclists are still dropped soon in the race it is unclear why this method performs this much better.

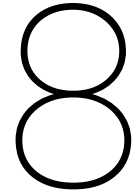


(a) Blocken



(b) Iniguez

Figure 7.1: The workload balance graph including the balancing strategies: no balancing, head times balancing, head times balancing with dropping and adjusted return positions, all corresponding to the optimisations performed using the CP physiological model



Conclusion

8.1. Model

In the analysis of the standard strategy and the optimisation of the new proposed strategies the model has shown that it gives good insights in the physiological states and power requirements during a team time trial. These power requirements and physiological states have been used to identify the cyclists in that are withholding the team from reaching higher mean velocities. The workload balances have been proven a good measure for how well the work is distributed in the group, which turns out to have a large influence on performance.

The differences in performance of cyclists that are simulated has a large influence on the optimal strategy. During this analysis standardised cyclists are used, however when real cyclists are tested it is important that the combination of their physiology and aerodynamics, resulting in the critical velocity is determined with accuracy.

The model lacks in validation, the combination of the mechanical and physiological model have been widely used in simulations of individual time trials[19, 24, 42, 45]. It is therefore that the only undetermined part of the model is the aerodynamic interaction. A lot of studies doing so with groups of four cyclists have been published[4, 10, 16, 18, 22, 29]. However the only two studies that have been published on the aerodynamic interaction in groups of up to eight cyclists have used poorly validated computational flow dynamics studies to do so. Since different strategies cause different results when using different aerodynamic models it is important that the aerodynamic interaction models are validated.

Even better then improving the validity of the aerodynamic interaction is to validate the models capability of estimating performance of a strategy. This could be done by comparing race results to the simulated result. This simulated result can be performed with the changing scheme that was used in the actual race.

Two physiological models have been used in this study however the different behaviour of the two models has not lead to a lot of differences in outcomes of strategies. The Margaria-Morton (MM) model could model a cyclist in more detail than the Critical Power (CP) model, however in this study it is not demonstrated that the different behaviour also resulted in different conclusions. It cannot be concluded that there is no advantage of using the MM model over the CP model since in this study the MM model is not fit to real cyclists, however when continuing with the standardised cyclists as presented in this model there is no advantage of using the MM model.

8.2. Strategy

During this study it is determined that the performance of the team time trial relies on the distribution of workload over the cyclists in the team. In this study the strategy was optimised for a group with large physiological differences among the team members. It is determined that when simulating with Blocken's aerodynamic model, the strategy can be improved such that the mean velocity over a team time trial is raised

by 0.358 m/s or 0.239 m/s for the CP and MM physiological models respectively. This is done by altering the return positions, such that every cyclist has its own designated position to return to instead of letting all cyclists return to the last positions, when changing from first. When simulating with Íñiguez's aerodynamic model, it was found that skipping worked best and was able to improve the mean velocity over the team time trial by 0.521 m/s simulated with the CP physiological model.

While remaining in the standard changing strategy, the order has proven to be of great influence to the results. When only using head times to balance a team during a team time trial the workload distribution is very dependent on the order that is used. It is found that between the best and the worst simulated orders the results expressed in mean velocity over a 30 km race ranges between 0.079 m/s and 0.228 m/s. The lowest improvement was found while simulating with the MM-Íñiguez configuration and the highest improvement was found while using the CP-Blocken combination.

9

Recomendations

The developed model is used to gain insights in the strategies used during team time trials and also to improve the strategies. The model has provided information regarding the workload among different cyclists in a team during the race and has helped develop new strategies that could potentially improve team time trial performances. However the model remains invalidated in this study. The model has been used to evaluate a single case, which is a flat time trial of 30 km with a single configuration of cyclists. The model has potential to evaluate a wide range of different cases. In this chapter will be explained both how the model could be improved and how the existing or improved model could be used to optimise more situations.

9.1. Model

A model of a team time trial was developed but it still lacks validity, also the model could be improved to simulate with higher detail. The aerodynamic models that are used in the different configurations of this model have shown very different behaviour. It is essential to determine which model suits the considered reality best.

9.1.1. Validation of the aerodynamic interaction

Since the two aerodynamic models show such a different behaviour and have lead to different conclusion in this study, a validation of the aerodynamic interaction has to be made. It is advised to do this in a field test while using power meters, since this method of assessment lies close to the use case in application. Alternatively a wind tunnel test could be done. It has been shown in A that it is also essential to do this with a larger groups size, at least five, but more preferable eight cyclists.

9.1.2. Individual aerodynamic characteristics

Recent studies [4, 18, 22] have also shown that the aerodynamic characteristics of the cyclists in the group have an influence on the coefficient of drafting that applies to the cyclists. During this study the considered cyclists were equal in size, however when a real time of different individuals is considered this will be important. The study of Heimans et al. (2017) provided a good framework that could be used to include the effect of different individual aerodynamic characteristics into the teams drafting model.

9.1.3. Additional aerodynamic improvements

The world of aerodynamics is more complex than drag areas and drafting coefficients, the applicability of the model would increase by including these details into the model. Winds are not included in this situation, the effects of head and tail winds can be included relatively easily, by separating forward velocity and air velocity. However when side winds are being considered this becomes more complex. When side winds occur in team time trials cyclists tend to introduce a lateral offset in their position in the group in order to remain drafting. It would be interesting to also include these effects in the model, such that the strategic decisions could be adapted to the weather conditions.

9.1.4. Overall performance validation

The aerodynamic interaction seems to be the least validated component of the model. However together with the physiology and resistance models it determines the time trial performance. The highest level of validation would be if it could be determined that the performance of this model would be accurate. This requires a fits of the desired physiological modes to a real team of cyclists, also the aerodynamic drag area and rolling resistances of these cyclists should be determined. This way a strategy of a real performed team time trial can be fed into the model and the performance can be compared to asses the model validity.

Relative validity With such large amount of parameters to determine, which in their way have inaccuracies the exact finish time will likely not match very accurate, however when multiple time trials are performed using different changing strategies. The differences in finish time or mean velocity can be compared to those of the model predictions. This way it could be ensured that the strategy optimisations by making use of the model will result in an improvement of performance in reality without predicting accurate finish times.

9.2. Studies using the existing model

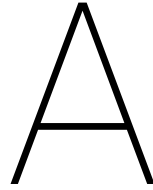
This study focusses on the development of a model to predict and compare performances in team time trials as well as optimising performance of the team time trial. Since this study contains much information about different model types and variation in strategies and group composition is decreased. A follow up study could provide much more information about the performance of strategies and different strategy concepts. In this section some ideas, which are currently labeled as interesting, are explained.

9.2.1. Performance difference on different slopes

In this study a few strategies have been analysed on a 30 km flat team time trial using only one group formation. There are still a lot of variation possible. In this section a few examples are given of additional cases that are expected to enrich this study with interesting results.

Order and inclination In the order optimisation no variation is made in cyclists weigh class or road inclination. It will be interesting to see how the optimal orders change with the inclination of the course. This can be done by taking the order that is now considered, which consists of two super strong cyclists, two strong cyclists, two medium and two weak and altering their weight. Specifically if the super strong cyclists become of the heavy weight class and the weak cyclists of light. This way depending on the road inclination the critical velocity of the cyclists change in the advantage of the weak cyclists and at the disadvantage of the super strong cyclists. This could even be performed with a course that has both a flat and inclining part.

More balanced groups The current considered group has a lot of variation between cyclists, which make the workload distribution important. It would be interesting to place in contrast to that a group where the cyclists are more balanced, for example six strong and two medium cyclists. It is expected that the strategies proposed to balance the workload have less effect in these cases, but it is unknown if they will perform worse, it could be that in cases that need less workload balancing these strategies may not have a large advantage, they still perform well.



Interpolation of cyclist drafting coefficient

This chapter describes the method of interpolation of drag reduction on cyclists in groups of various sizes, where the goal is to get drag reductions for a group of any number of cyclists. Two studies have been performed where the aerodynamic interaction of groups of eight cyclists have been tested, both lack validity. The study of Íñiguez and Íñiguez de-la-Torre (2009) [27] tested the drafting coefficients of all group sizes up to nine. The study of Blocken et al. (2013) [9] tested only with group sizes 1, 2, 4, 6 and 8 More studies have been performed on configurations with four cyclists also varying individual drag areas and postures. In order to use both studies for up to eight cyclists an interpolation has to be performed use all cyclists configurations. Possibly the same method of interpolation could be used to extrapolate the drag reduction in groups of four cyclists to groups of eight cyclists. This study attempts to describe the drafting coefficients of a group, but often the drag reduction is mentioned. With the drafting coefficient (C_{dr}), the drag in the group with respect to the solo drag value is meant. The relative drag reduction (R) is the ratio between drag difference between solo and in group and the solo drag value and is related to the drafting coefficient as described in equation A.1.

$$R = 1 - C_{dr} \tag{A.1}$$

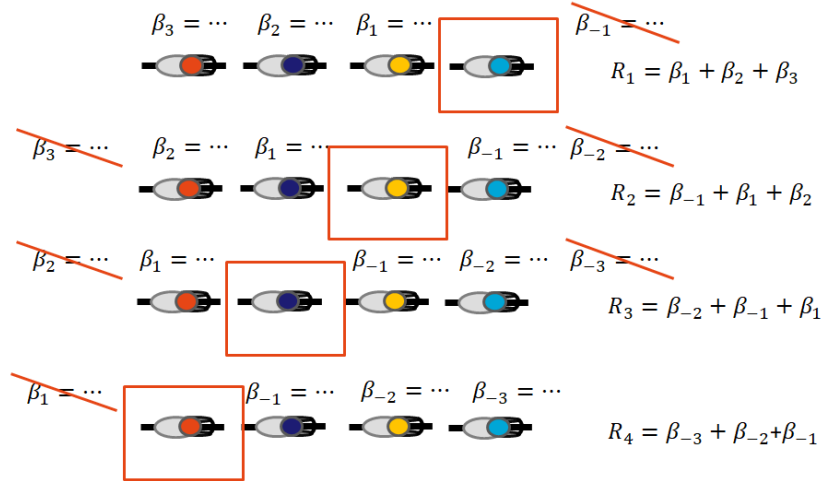


Figure A.1: This figure shows the working principal of the explained method, the coefficients (β) are placed above the cyclists, the relative reduction coefficient for each row corresponds to the boxed cyclist.

A.1. Method

In this section a mathematical framework is presented on how the drafting coefficient is related to the position in the group when the group is in an in-line formation and how it is used to estimate the coefficients in groups of sizes which are not tested. An in-line formation means that the cyclists are cycling after each other, where the rear wheel of a leading cyclist is followed by the front wheel of a trailing cyclist. In this analysis the effects of side winds and misalignments in the group are neglected.

A.1.1. Framework

Let a group of cyclists consist of (N_{Group}) cyclists travelling in in-line formation, the drag reduction of any cyclists in the group is considered dependent on the amount of cyclists in front of the cyclist as well as the amount of cyclists trailing behind this cyclist. The total drag reduction of a cyclist is described as the sum of the contributions of the considered cyclists around him. The amount of cyclists that contribute to the drag reduction is as a number of cyclists in front of the evaluated position N_{front} and a number of cyclists behind the evaluated cyclist (N_{rear}). A configuration is denoted by: (N_{front}, N_{rear}). The total reduction for a cyclist is described by the sum of the drag reduction contributions (β) of the relative positions for all positions that are occupied in the region between N_{front} in front and N_{rear} behind the cyclist, as shown in equation A.2a. In this equation the factor $\psi(i, j)$ determines the existence of a cyclist in the relative position j with respect to the cyclist in position i , as described in equation A.2b.

$$R_i = \sum_{j=-N_{front}}^{N_{rear}} \beta[j] \cdot \psi(i, j) \quad (\text{A.2a})$$

$$\psi = \begin{cases} 1 & i - j > 0 \cap i - j \leq N_{group} \cap i \neq j \\ 0 & \text{otherwise} \end{cases} \quad (\text{A.2b})$$

Equation A.2 can be written into matrix form. Here the vector β can represent the drag reduction contributions of the cyclists in the positions around the evaluated cyclists, meaning first the contributions of all cyclists which are in front followed by the contributions of the cyclists behind the evaluated cyclist. If the values for $\psi(i, j)$ are brought into a matrix Ψ_{ij} , the presence matrix, the drag relative drag reductions (R) can be produced by equation A.3.

$$\mathbf{R} = \Psi \beta \quad (\text{A.3})$$

This paragraph will give an example on how to use the explained equation. A group of four cyclists is considered ($N_{group} = 4$), the influence of drafting is determined by the presence of cyclist in the three positions in front ($N_{front} = 3$) and three positions behind ($N_{rear} = 3$), or configuration (3,3). The presence matrix is shown in equation A.4. In this matrix the rows correspond to the relative drag reduction factors of a position, the first row is for the first cyclist, the second for the second cyclist and so on. The first three columns correspond to the positions in front of the evaluated cyclists, where the first is the furthest away from the evaluated cyclist and the third, the one directly in front. The last three columns correspond to the following positions directly after the evaluated cyclist. As presented for the first cyclist there are no cyclists in front and three cyclists behind the evaluated cyclist. The vector containing the contributions to relative drafting reduction (β) has rows that correspond to the positions the same as the columns of the presence matrix, such that the multiplication results in the relative drag reduction for all positions.

$$\Psi = \begin{bmatrix} 0 & 0 & 0 & 1 & 1 & 1 \\ 0 & 0 & 1 & 1 & 1 & 0 \\ 0 & 1 & 1 & 1 & 0 & 0 \\ 1 & 1 & 1 & 0 & 0 & 0 \end{bmatrix} \quad (\text{A.4})$$

A.1.2. Least squares estimation

In this section the estimation of the drafting coefficient of the missing group sizes of Blocken's aerodynamic interactions study using a least square estimation. The study of Blocken describes groups with 1, 2, 4, 6 and 8, totalling in 21 drafting coefficients. For each of these drafting coefficients a row in the presence matrix can be created, with a corresponding relative drag reduction. The equation where the relative drag reduction is estimated is shown in equation A.5a, here the set ϵ represents the error in the estimate $\Psi\beta$. The coefficients β can be solved using least squares, as presented in equation A.5b in which the squared error ($\epsilon^T\epsilon$) is minimised.

$$\mathbf{R} = \Psi\beta + \epsilon \quad (\text{A.5a})$$

$$\beta = (\Psi^T\Psi)^{-1}\Psi^T\mathbf{R} \quad (\text{A.5b})$$

Amount of coefficients The amount of coefficients that are used are important to the result, also whether the positions in front or behind the cyclists are considered, are important. There are 21 drafting coefficients known, this means that the maximum of 14 coefficients (7,7) is over constraint and can be used, however it might be that some coefficients have little influence. First the error in the fit is tested for all possible coefficients. After this a lower number of coefficients is selected to see how it changes the behaviour of the fit. Also a fit is made to the data of just the test with four cyclists, to see how it fits if extrapolated to larger group sizes.

Table A.1: The sum of squared error from the fits made to all tests from Blocken et al. (2013) [9], the columns represent the number of coefficients considered belonging to positions behind the cyclist and the rows the number of coefficients belonging to positions in front of the cyclists.

		cyclists behind							
		0	1	2	3	4	5	6	7
cyclists in front	0		16.18 %	16.15 %	51.73 %	15.67 %	15.37 %	15.35 %	15.17 %
	1	6.21 %	6.11 %	5.93 %	5.91 %	5.75 %	5.75 %	5.70 %	5.43 %
	2	3.38 %	3.21 %	3.21 %	3.14 %	3.14 %	3.13 %	3.03 %	3.03 %
	3	2.29 %	1.64 %	1.62 %	1.62 %	1.61 %	1.56 %	1.56 %	1.56 %
	4	1.83 %	0.87 %	0.86 %	0.86 %	0.84 %	0.83 %	0.82 %	0.82 %
	5	1.80 %	0.61 %	0.61 %	0.60 %	0.60 %	0.60 %	0.60 %	0.59 %
	6	1.75 %	0.43 %	0.36 %	0.36 %	0.36 %	0.34 %	0.33 %	0.31 %
	7	1.75 %	0.27 %	0.25 %	0.25 %	0.25 %	0.22 %	0.21 %	0.18 %

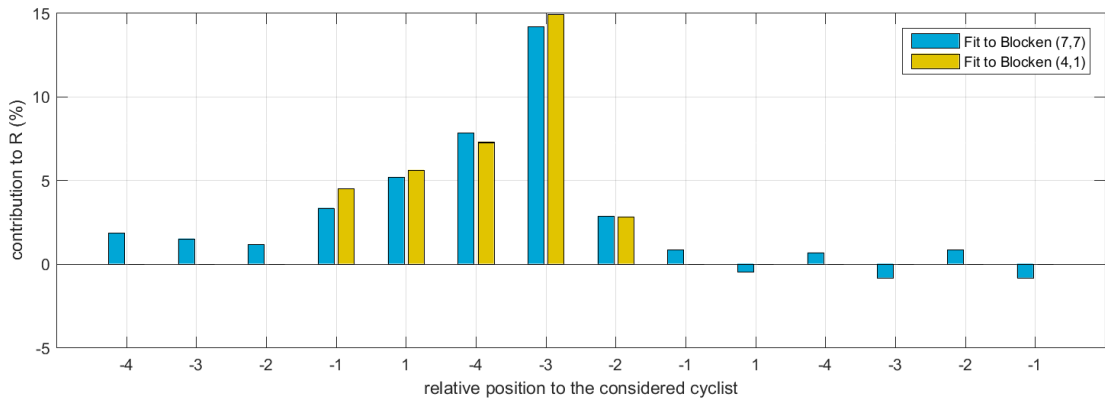


Figure A.2: The coefficients contributing to the drafting for configurations (7,7) and (4,1).

A.2. Results

The results are separated in two parts, the interpolation in groups up to eight and in the extrapolation of the drag reduction of a group of four, to groups of eight. With the interpolation all data from Blocken's aerodynamic interaction study are used, to define the drafting coefficients in not tested group sizes. With the extrapolation, from both Íñiguez and Blocken, the test with four cyclist is used to replicate all other group sizes in order to determine whether this could also be done in studies that do not have data from larger group sizes.

A.2.1. interpolation in groups up to eight

Multiple configurations of coefficients have been fitted to the data, the configurations (7,7) and (4,1) are highlighted, as well as the case with three in front and one behind for the estimation for a group of four cyclists. The RMS error for all configurations of coefficients, fitted to all available data from Blocken's study, are presented in table A.1. It is noticeable that with considering contributions of at least three cyclists in front and one behind, the RMS error is lower than 1 %. It is also shown that the contribution of considering a cyclist, in front of the cyclists, to the accuracy is much larger than that of a cyclist, behind the cyclist of which the drag reduction is computed. However an extra coefficient will always increase the accuracy. The coefficients of the most accurate fit (configuration (7,7)) are compared to the original drafting coefficients and are presented in figure A.1. The complete table of drafting coefficients is presented in table A.2, within the accuracy of 1 % none of the coefficients of the original tests deviated from the reproduced value.

As mentioned earlier it might not be necessary to use all coefficients possible, therefore a comparison is made between the configuration with the maximum amount of coefficients and one with less coefficients, which is chosen to be configuration (4,1). The coefficients for configurations (7,7) and (4,1) are presented in figure A.2. The coefficients are remarkably similar, as are the resulting drafting coefficients for groups of 2, 4, 6 and eight cyclists, which is presented in figure A.3.

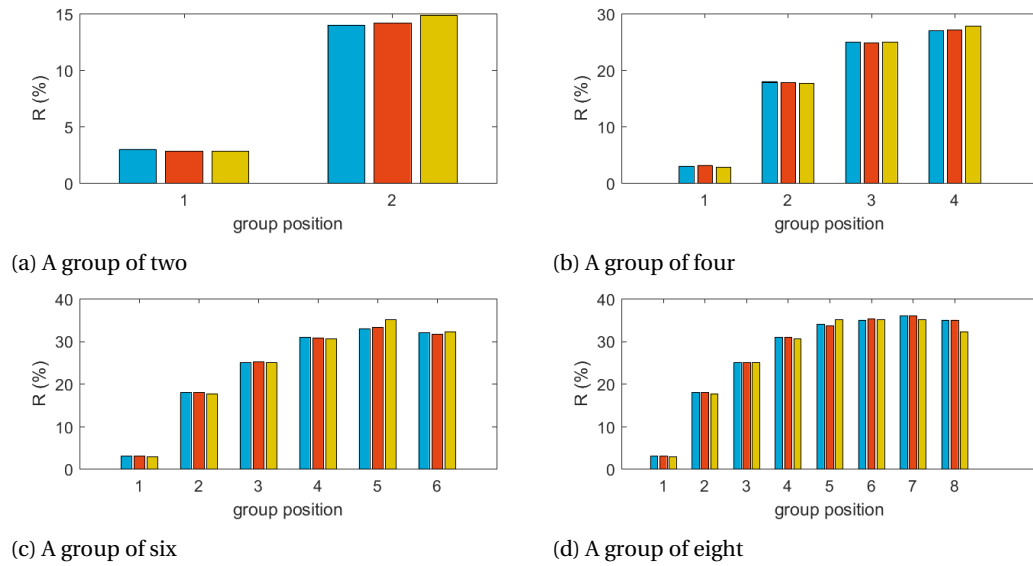


Figure A.3: The drag reduction coefficients of cyclists in groups of 2 (a), 4 (b), 6 (c) and 8 (d) cyclists, for both original study of Blocken and fit from (7,7). «Maybe delete A.3 and include both (7,7) and (4,1) into these plots.»

Table A.2: Drafting coefficients from the fit with configuration (7,7). All coefficients of the tested data are exactly equal to the reproduced data, when rounded to 1% accuracy.

Gr. Size	C_{dr1}	C_{dr2}	C_{dr3}	C_{dr4}	C_{dr5}	C_{dr6}	C_{dr7}	C_{dr8}
1	100							
2	97	86						
3	97	83	78					
4	97	82	75	73				
5	96	82	75	70	70			
6	97	82	75	69	67	68		
7	96	82	75	70	66	66	67	
8	97	82	75	69	66	65	64	65

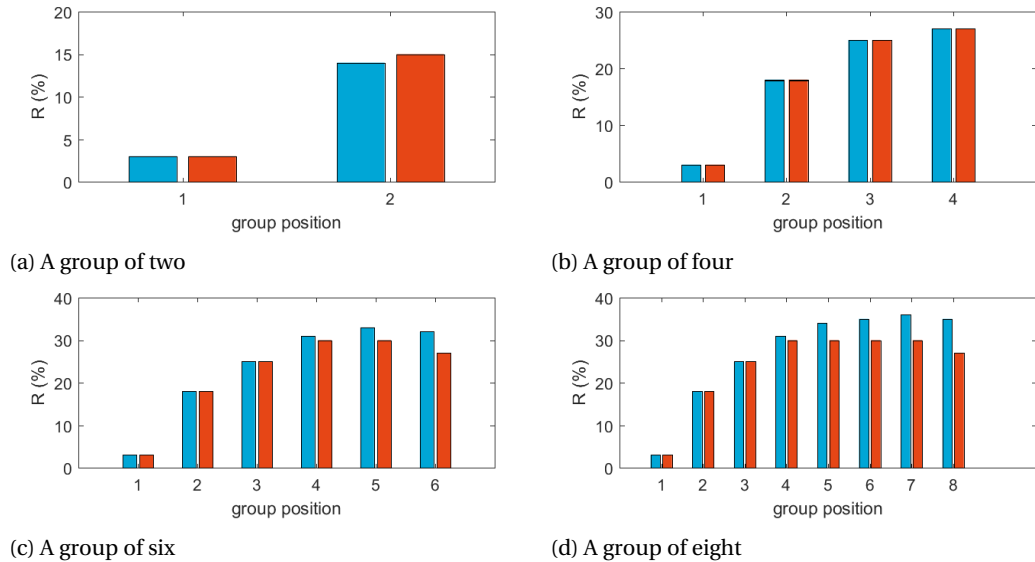


Figure A.4: The relative drag reduction coefficients, test data from Blocken [9] (light-blue), versus the fit (3,1) from a group of four cyclists (red).

A.2.2. Extrapolation from a group of four cyclists

Two fits are made to the tests with four cyclists from both Íñiguez and Blocken, the resulting fits to the other group sizes are presented. The fits to Blocken's tests with two, four, six and eight cyclists are presented in figure A.4. Since the fit that is made uses four coefficients, and therefore has four degrees of freedom, the fit to four cyclists is exact (RMS error = 0). In the cases with more cyclists it is shown that the fit has lower drag reduction. The fit to the coefficients of Íñiguez's study is presented in figure A.5. As with the fit to Blocken's coefficients the drag reduction coefficients from the fit are exactly equal for four cyclists and have only small errors for two cyclists. In the cases with six and eight cyclists the fit is somewhat flattened; with which is meant that the difference between coefficients is lower in the fit, than the differences from the coefficients from the study.

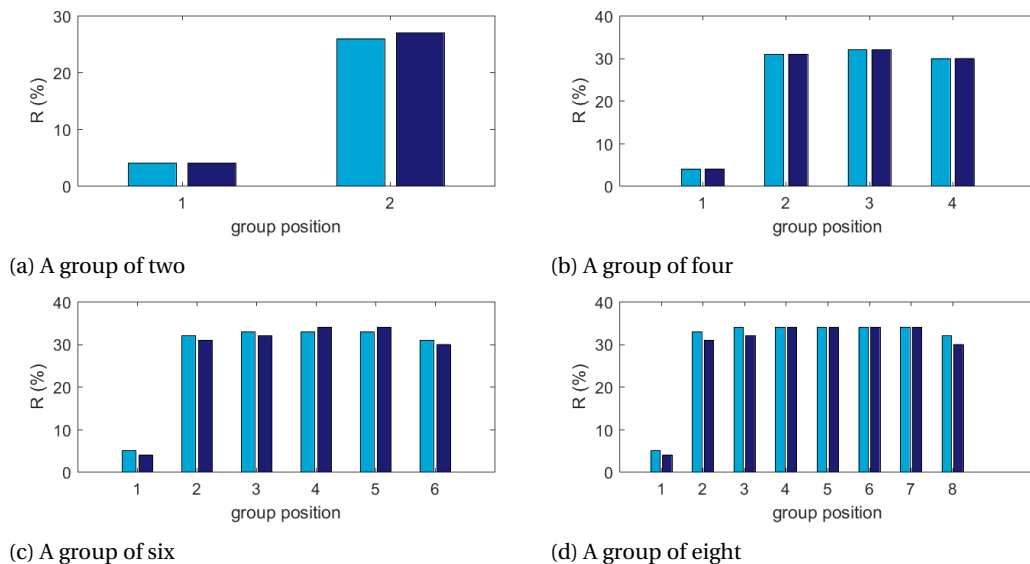


Figure A.5: The relative drag reduction coefficients, test data from Íñiguez [27] (light-blue), versus the fit (3,1) from a group of four cyclists (dark-blue).

A.3. Discussion

...

The RMS error in the coefficients as presented in A.1 are relatively low, this is because all tests from Blocken are considered, including one cyclist, and two cyclists. The test with one cyclist will according to the framework always return that there is no drag reduction. The test with more cyclists will have more deviation in the drafting coefficients of cyclists beyond fourth position. This can be explained since the relative drag reduction coefficients, from the Blocken's coefficients in a group of eight to those of the fit in configuration (7,1), shows only deviations larger than 0.5 % in positions five and six. The coefficients of configuration (4,1) has more deviations, where the drag reduction coefficients corresponding to positions five seven and eight exceed 0.5 % in absolute error.

For the extrapolation only using a test with four cyclists to determine the drag reduction factors, the results show an RMS error to all tests of 2.9 % and 1.1 % for Blocken and Íñiguez respectively. The differences in relative power output (which is closely related to the drafting coefficient) are shown in figure A.6, with respect to those differences the 2.9 % and 1.1 % are not large. The RMS error might suggest that the fit is performing well, however when looking at the graphs figure A.4 it is shown that the behaviour is different. The estimated drag reductions in cyclists in the back (position beyond fifth) of large groups (>4). The data of Íñiguez has deviations that are most present in positions two and three of large groups (>4), which also seems like a structural error.

A.4. conclusion

The missing coefficients of drag reduction from Blocken's [8] drag reduction study were estimated by relating a contribution to the reduction to each occupied positions around the cyclist. Many configurations were tested, where they varied in how many positions in front and behind the cyclists were considered to contribute to the reduction. The most accurate fit was found where all seven positions in front and all seven positions behind the cyclists were considered. In this case the RMS error over all test with groups of 1, 2, 4, 6 and 8 cyclists is 0.18 % with this case. It was found that any configuration using at least four cyclists in front and one behind works well as well, with an RMS error over all tests of 0.87 %. It was shown that both of these examples showed a similar profile in drag reduction over the positions in the group, which was also in correspondence to the original experiments.

It was suggested that the fit to data of the tests performed with four cyclists could predict the behaviour in drag reduction in groups up to eight cyclists. This was tested by making a fit to the results of the tests from both Íñiguez [27] and Blocken [9] with only four cyclists and comparing the resulting drag reduction of

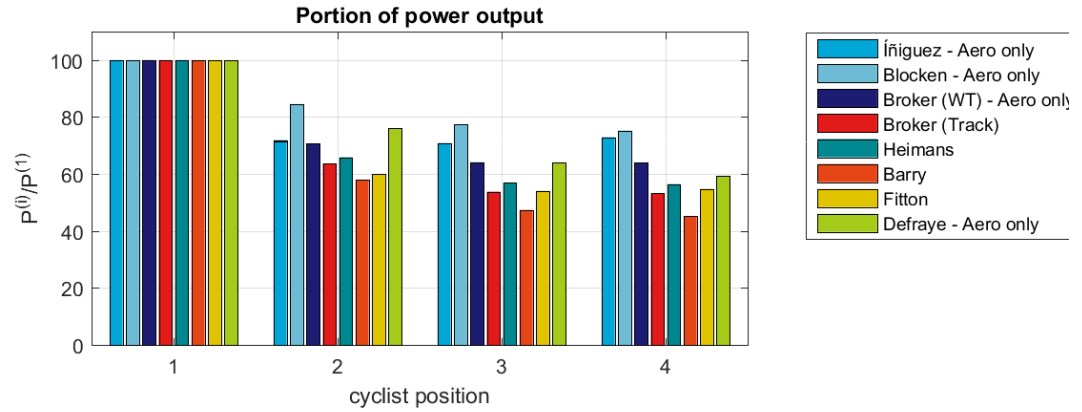


Figure A.6: Comparison of drag reduction, in terms of ratio in power consumption with respect to the first cyclist in the group, as function of group position coefficient for groups of four cyclists.

all group sizes to the tests. The RMS errors in the drafting coefficients were 2.9 % and 1.1 % respectively. It was found that the errors were largest in the positions beyond fourth for groups larger than four for Blocken's study. In the case of the fit to Íñiguez's coefficients the errors were largest in positions two and three in groups larger than four. It is shown in A.4 that the profile of drag reduction over positions in the group is altered when interpolating from a group of four cyclists, and it is therefore concluded that it cannot be guaranteed that this gives a representative result. The profile of drag reduction and thereby drafting coefficient over the positions is important when comparing different strategies, disturbing this profile might induce advantage of certain strategies.

B

Fitting the Margaria-Morton models

B.1. Introduction

In the literature the critical power model (CP-model) [30] is often used to model physiology, while the Margaria-Morton model (MM-model) [33, 41] could give more detail than the critical power model. The reason that the CP-model is so popular with respect to the MM-model is because it only uses two parameters, which is far less than the eight used in the MM-model. Because the MM-model, describes the physiology in more detail with respect to the CP-model it has potential to describe the complex physiology in team time trails better than the CP-model.

The critical power model is often used in the modelling of individual time trials [14, 42], however in these studies, no recovery of anaerobic capacity is required. Since team time trials are an intermitted exercise, meaning that the power output of a cyclist fluctuates around the critical power, the model has to model recovery. The accuracy of the CP-model decreases when using a recovery model. [5, 44] It is therefore suggested that the hard to fit MM-model could provide a better description of the cyclists ability to produce power.

B.2. The MM-model

The MM-model is a whole body bio-energetic model, where processes leading to power production are described based on bio-chemical processes. The MM-model is often represented in a hydraulic flow model, where flows represent power and volumes represent energy. The hydraulic flow model representation is shown in figure B.1, where the three tanks are noted with O, P and G. The O-tank represents the oxidative production of phosphates, which are used in the production of mechanical power. The O tank is infinite in size, representing the oxygen in the environment. The P-tank represents the storage of ATP, and the G tank represents the storage of carbohydrates, which supply energy to tank P through the glycolysis process. During the glycolysis process, lactate is converted to lactic acid.

B.2.1. Differential equations

The MM-model is, in literature, described as a hydraulic flow model, however the result of this model are only differential equations. The main differential equations are the two equations related to the change of height in the tanks, shown in B.1a and B.1b. In these equations, there is a reference to powers P1 refers to the power through R1 from tank (O to P), P2 is the power through R2 (G to P), P3 is the power through R3 (P to G). The athletes power output is represented by P_{out} . These powers are dependent on resistances and hight difference, but only under certain conditions and are therefore defined in B.1.

$$C_p \cdot \frac{dh_p}{dt} = -P_{out} + P1 + P2 - P3 \quad (\text{B.1a})$$

$$C_g \cdot \frac{dh_g}{dt} = -P2 + P3 \quad (\text{B.1b})$$

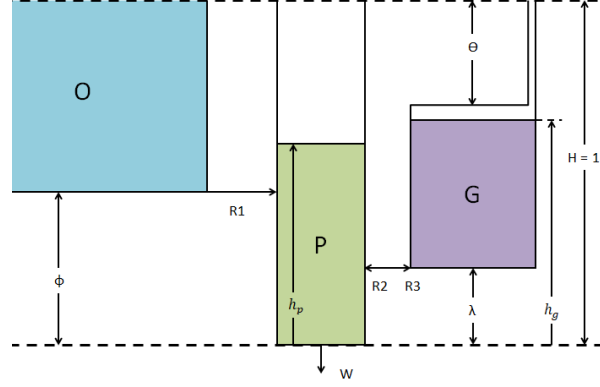


Figure B.1: Hydraulic flow representation of the generalised MM model.

Table B.1: Equations for the energy flows

value	condition
P1	
$P_1 = \frac{1-h_g}{R_1}$	$h_p > h_O$
$P_1 = \frac{1-h_O}{R_1}$	$h_p \leq h_O$
P2	
$P_2 = \frac{h_g-h_p}{R_2}$	$h_p < h_g \cap \lambda < h_g < 1-\Theta$
$P_2 = 0, h_g = h_p$	$h_g \geq 1-\Theta$
$P_2 = \frac{h_g-\lambda}{R_2}$	$h_p \leq \lambda$
$P_2 = 0, h_g = h_p$	$h_p \geq h_g$
P3	
$P_3 = \frac{h_p-h_g}{R_3}$	$h_p > h_g \cap 1-\Theta \geq h_g \geq \lambda$
$P_3 = 0, h_g = h_p$	$h_g < 1-\Theta$
$P_3 = 0$	$h_p < \lambda \cup h_p < h_g$

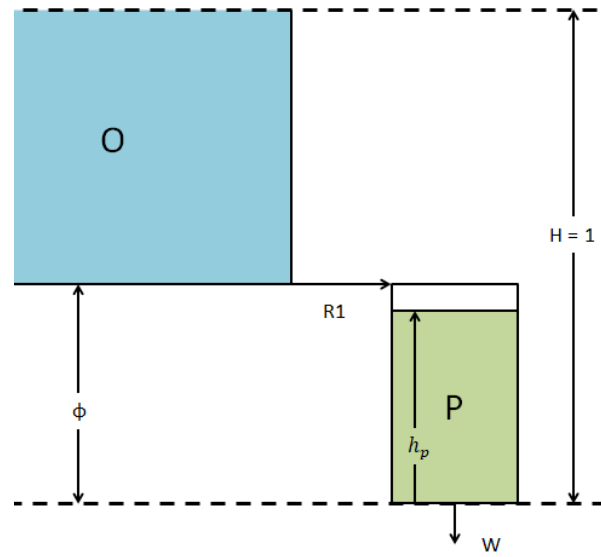


Figure B.2: CP-model as an MM-model in hydraulic flow representation.

For the CP-model, the differential equations are different. There is only one state (W_{Bal}) and two parameters (CP and W'). The differential equations are shown in B.2 where Bartram's recovery equation is used. [5]

$$\frac{dW_{Bal}}{dt} = \begin{cases} P - CP & P \geq CP \\ \frac{W' - W'_{Bal}}{2287.2 \cdot (CP - P)^{-0.688}} & P < CP \end{cases} \quad (B.2)$$

The model uses three relative sizing constraints (Φ , λ , θ), the capacities of both tanks and three resistances of the energy flows between tanks (C_P and C_G). Of the resistances $R1$ determines the aerobic power, $R2$ the power from the glycolysis process and $R3$ the recovery of glycolysis. There are two physiological states, these are the heights of the tanks in hydraulic flow representation and can directly be related to the fullness of the reserves.

The height differences between tanks will trigger the flow through the tubes, which have a resistance. When there is power output the level of tank P will lower, triggering flows from O and G into tank P, proportional to the level differences. The resistances determine the flow rate per level difference (lower resistance gives a larger energy flow).

B.2.2. Sizing

The relative sizing constants will determine for a large part the characteristics of the model. When the level of P first reaches beneath the top of tank G, lactic acid is produced, meaning that the power output at a steady state, where the level of P is at the top of G represents the anaerobic threshold. The same can be done for critical power, in this case the levels of both P and G are at steady state at the bottom of tank O.

It is, with some alternations, possible to the critical power model exactly, this is done by removing the tank G and setting a top limit on tank P exactly at the level of the bottom of tank O, as shown in B.2. While maintaining the tank G and not lowering the top of tank P, the same result is approached when $R1$ reaches zero, while the maximum aerobic flow remains CP , see B.3.

$$R1 = \lim_{\Phi \rightarrow 1} \frac{1 - \Phi}{CP} \quad (B.3)$$

B.3. Method

In literature there is a lack of information and standardisation on how to fit a MM-model to an athlete. That combined with the lack of resources to perform the required test to do so, makes for an easy decision to provide parameters for fictional cyclists. A combination of tests that could also be used to fit the critical power model are combined with a test that of intermittent exercise, to determine the recovery kinetics.

In this study, standardised cyclists are used, the parameters of the critical power model, for the standardised cyclists, are used to generate those for the MM-models of the same fictional cyclists. The two constants of the CP-model are, critical power and anaerobic work capacity. Those two are proportionally scaled along the standardised cyclists, which are shown in equation B.2.

Table B.2: Standardised physiological coefficients in strength classes for the CP-model.

Power class	CP	W'
	W	kJ
Super strong	450	25.0
Strong	420	23.3
Medium	390	21.7
Weak	360	20.0

B.3.1. constraints

The MM-model can be configured in various configurations, the desired configuration is such that it shows a different behaviour with respect the the CP-model. Having two models that have different characteristics, different optima in strategies might be found according to the model which is used. To make the model different from the CP-model the relative sizing coefficient Φ is chosen to be low (0.2). It is assumed that the anaerobic threshold for this athlete is at half of the critical power leading to $\theta = 0.4$. The coefficient λ is set to 0.1. In order to model that the G reserve is actually used, the size of the P tank is set to exactly half of the W' reserve in the corresponding CP-model. This leaves four constants undefined, which could be fitted with a minimum of four tests.

B.3.2. Tests

Because using the constraints, four constants of the MM-model are undefined, four tests are done to fit the MM-model to the CP-model. The CP-model can be fitted to cyclists using a series of three self paced all out tests. [6] The duration of these tests are set to one, three and twenty minute tests. The last test is an intermittent test as performed in the study from Bartram's recovery model. [5] Using these tests, the model parameters are fitted such as they would in a test to determine the parameters for the critical power model. The power profiles of the tests are shown along with the results in B.3

B.3.3. Optimisation

The parameters were adjusted manually, after which a gradient optimisation was performed to find the local minimum to this problem. Optimisation was performed using the 'trust-region-reflection' algorithm. The optimisation was performed in MATLAB using default settings of the 'fmincon' function.

The objective is that the at all tests the tank is first empty exactly at the end of the test. The scores of the tests are combined by taking the root mean square of the individual test errors, as defined in equation B.4b. The individual test are simulated with a fixed time step simulation. If the value for h_P would reach below zero, the simulation is terminated and the time of failure (t_{fail}) is computed, the error in time between failure and objective is the objective score. If the simulation is valid the remaining level in the tank P ($h_P[end]$) is the objective score, as shown in equation B.4a.

$$er_i = \begin{cases} h_P[end] & \min(h_P(t)) \geq 0 \\ \frac{t_{objective} - t_{fail}}{t_{objective}} & \min(h_P(t)) < 0 \end{cases} \quad (\text{B.4a})$$

$$J = \sqrt{\sum_{i=1}^4 er_i^2} \quad (\text{B.4b})$$

The relative sizing parameters (Φ , λ and θ) are not scaled for the other strength classes, all other parameters are scaled proportional to the critical power of the CP-model of the same strength class. This way only one strength class is optimised. In case of the possibility of multiple optima, this makes sure that all strength classes use the same optimum. The optimisation is performed on the strength class 'Strong'.

B.4. Results and discussion

Using the optimisation the results are produced and shown in table B.3, in this table the resistances are converted to an admittance (D , $D = R^{-1}$), which represents the energy flow per tank level difference. What surprises is the value for $D1$, in strength class Super Strong it has a value of 577.1 W, multiplying this with the level difference between top of tank P (1) and the bottom of tank O ($\Phi = 0.2$), this results in the maximum aerobic power and is equal to 461.7 W, see B.6. The maximum aerobic power of the MM-model is thereby 11.7 W (2.6 %) higher than the critical power of the same strength class. The higher maximal aerobic power can be explained by the fact that when the athlete is at steady state power output at maximal aerobic power, using the relative sizing parameters chosen, very little anaerobic capacity is left. The additional bit of aerobic power compensates for the lack of anaerobic work beyond this point, in longer endurance tasks such as the twenty minute test or the intermittent test. Also the total anaerobic work capacity is over four times as large as the W' of the CP-model (103 kJ for MM and 25 kJ for CP). The reason for this effect is that a large part of the G reserve is consumed when aerobic power is low, meaning that with the MM-model a lot of the anaerobic energy is consumed while the aerobic power is below maximal aerobic power. With the CP model when the power output is below maximum aerobic power, the whole power output is considered aerobic.

$$P_{O2,max} = D1 \cdot (1 - \Phi) \quad (B.5)$$

$$W_{an,MM} = C_P + C_G \cdot (1 - \lambda - \theta) \quad (B.6)$$

Table B.3: Standardised physiological coefficients in strength classes for the CP-model.

parameter	units	Weak	Medium	Strong	Super Strong
Φ	-	0.2	0.2	0.2	0.2
λ	-	0.1	0.1	0.1	0.1
θ	-	0.4	0.4	0.4	0.4
$D1 = R1^{-1}$	W	461.7	500.1	538.6	577.1
$D2 = R2^{-1}$	W	1290	1398	1505	1613
$D3 = R3^{-1}$	W	960.0	1040	1120	1200
C_P	kJ	10.00	10833	11.67	12.50
C_G	kJ	72.72	78.78	84.84	90.90

The errors of the four test and the resulting objective value are shown in table B.4, the values are low and surprisingly similar between strength classes. The low values mean that the optimisation yielded a good outcome that fits all four tests well. The similarity among strength classes means that fitting just one strength class and scaling up and down to the other strength classes was a successful choice, now all strength classes contain the same error as the fitted class.

Table B.4: Standardised physiological coefficients in strength classes for the CP-model.

Error values	er_1	er_2	er_3	er_4	J
Weak	$2.10 \cdot 10^{-5}$	$9.89 \cdot 10^{-4}$	$1.80 \cdot 10^{-2}$	$7.93 \cdot 10^{-5}$	$9.84 \cdot 10^{-3}$
Medium	$1.90 \cdot 10^{-5}$	$9.75 \cdot 10^{-4}$	$1.79 \cdot 10^{-2}$	$3.18 \cdot 10^{-3}$	$9.10 \cdot 10^{-3}$
Strong	$1.70 \cdot 10^{-5}$	$9.63 \cdot 10^{-4}$	$1.78 \cdot 10^{-2}$	$6.82 \cdot 10^{-4}$	$3.88 \cdot 10^{-3}$
Super Strong	$3.88 \cdot 10^{-5}$	$9.53 \cdot 10^{-4}$	$1.78 \cdot 10^{-2}$	$4.23 \cdot 10^{-5}$	$8.90 \cdot 10^{-3}$

The results of a simulation are the physiological states, for all test were the fit is optimised to the physiological states are plotted against time. This is done considering a cyclist of strength class 'Strong', where the mass is not influential. In the figure, the plots on each row represent a test, where on the left (plots a, c, e and g) the reference is plotted, this consists of the power profile and the W_{Bal} (physiological stat of the CP model). On

the right side (plot b, d and h) the results are plotted of the fitted MM-model, these are the reserve levels (h_P and h_G).

In the first three tests expenditure was tested only, by comparing the CP-model results and MM-model results, it can already be seen that the behaviour is quite different. In figure B.3 the plots in a, c and e show both power and the W_{Bal} state of the CP-model, these last are all straight lines. When looking at the MM-states in figure B.3 plots b, d and f, the lines are curved. When both tanks are full, the aerobic supply of power is zero, later when reserve P is slightly depleted, the oxidative power input will decrease the rate of depletion for reserve P. Later the flow from G to P will have the same effect, until the level in reserve G will approach its bottom, than the flow from G to P stops and the depletion of reserve P speeds up, as can be seen in the two longer tests in figure B.3 d and f.

Looking at the intermittent test (B.3: g and h) the states of both models might appear different, but they show quite similar behaviours. It is shown that using the MM-model h_P and h_G first decline during the first section of relatively low power output. At these lower values the recovery takes place. The W_{Bal} state from the CP-model also shows more recovery when depleted further. Because of the chosen configuration of the MM-model, the recovery of h_P , glycolytic processes (G reserve) as oxidative processes (O reserve), the recovery only gets high when the h_P level approaches the bottom.

In figure B.4 plots are made for three cases of intermittent exercise, for each case the left plot indicates the power profile, the middle plot, the states of the MM-model and the right plot the state of the CP-model. The test are with different ratios of high power and rest power. What can be noted from the plots is that for short peaks of power output the CP-model predicts better performance. This can be seen, because in figure B.4 (a), the h_P state from the MM-model is empty at the end, while the W'_{Bal} state from the CP-model is not. In plot figure B.4 (b) there is a slight difference in advantage of the CP-model, but they are somewhat equal in performance. Considering, long rests and short power peaks as shown in figure B.4 (c), the MM-model predicts better performance than the CP-model. This is of course in the case of an MM-model configuration as fitted as in this report.

While the previous paragraph reports a different behaviour of the MM-model with respect to the CP-model, it must be noted that the CP-model is already a generalisation of the human performance. The CP-model has only two degrees of freedom, while it uses at least three tests to be accurately fitted. [6] Additionally the recovery model used in combination with the CP-model is generalised over multiple subjects. [5] If the MM-model would have been fitted to an athlete performing real tests, this might give an MM-model that shows an even more different behaviour than the MM-model fitted to fictional tests. It would therefore be a good addition to this study to provide a MM-model specifically fitted to an athlete. More specifically it would be good to fit an MM-model to multiple cyclists, to show the different characteristics among them and the effect of it on their team time trial characteristics.

B.5. conclusion

A version of the MM-model is fitted to fictional tests, of which the outcomes are predicted by the CP-model. A configuration of the MM-model is assumed where it is expected to show a different behaviour with respect to the MM-model. It has been shown that to recovery of different duration it does indeed show a different behaviour with respect to it's CP-model counterpart. It could be that when fitted to a real athlete, the characteristics will even differ more among the two models, since the CP-model is generalises the cyclists a lot.

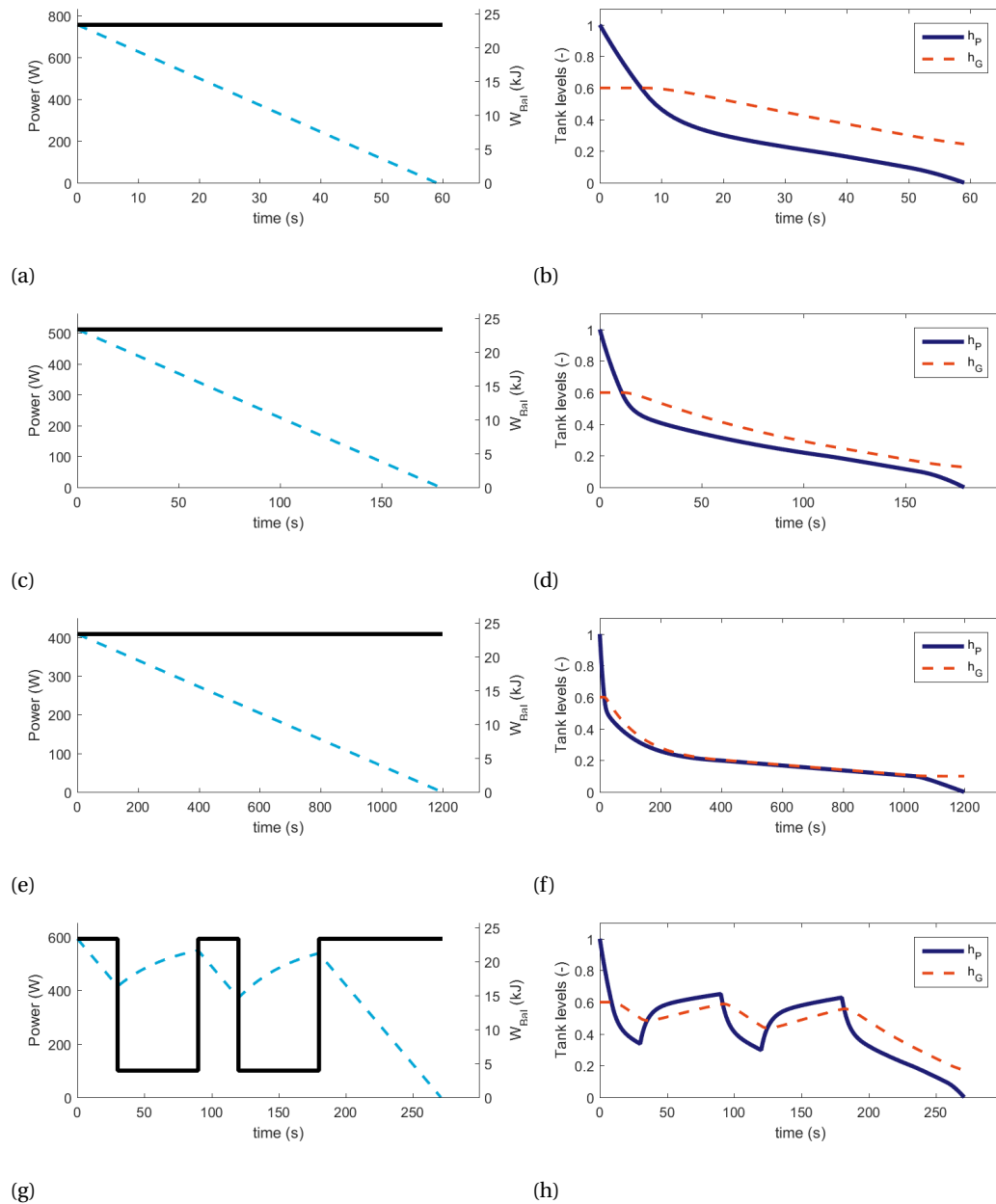
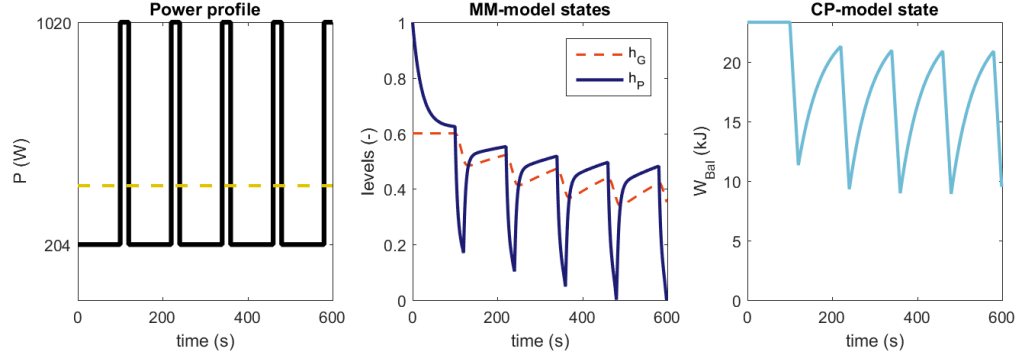
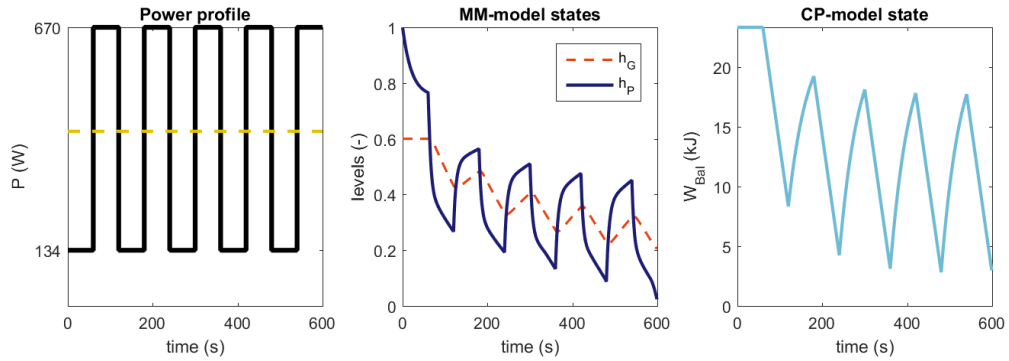


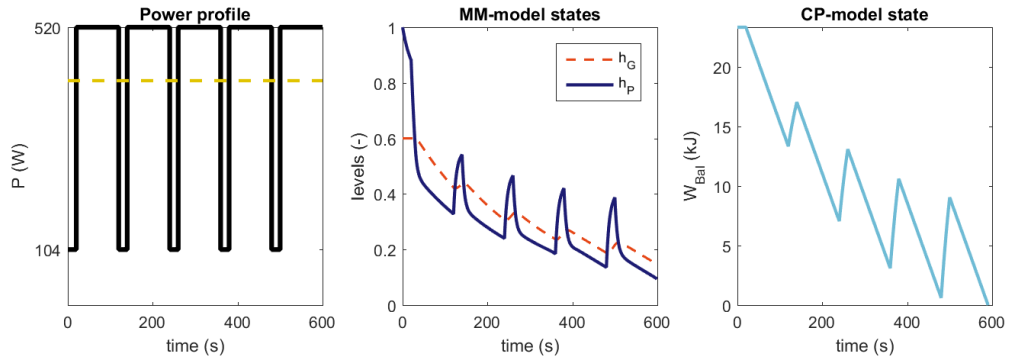
Figure B.3: The fitted MM-model for the standardised strength of the strong cyclist. in the left plots the power output of the test is shown (solid) along with the W_{Bal} state of the simulated CP-model. In the right plot the physiological states in form of the tank levels are shown corresponding to the simulated test with the MM-model. Plots a and b are from the one-minute test, c and d are from the three minute test, e and f are from the twenty minute test and g and h are from the intermittent test.



(a) Intermittent exercise with short power and long recovery while $P_{peak} = 1020W$.



(b) Intermittent exercise with medium power and medium recovery while $P_{peak} = 670W$.



(c) Intermittent exercise with long power and short recovery while $P_{peak} = 520W$.

Figure B.4: Plots of physiological states of both models in three different intermittent exercises, the ratio between power and recovery time are varied. The power ratio $R_p = \frac{P_{rest}}{P_{peak}}$ is 0.2. In the plots shown in (a) rest is long (100 s) and power is short (20 s), in (b) power and rest phase are of medium duration (60 s), in (c) the rest is short (20 s) and power is long (100 s). For each cases the left plot is the power output (solid line is power output, the dashed is critical power), the center plot are the states of the MM-model and the right plot shows the state of the CP-model.

Bibliography

- [1] Bicycle rolling resistance: The test. <https://www.bicyclerollingresistance.com/the-test>. Accessed: 20-07-2018.
- [2] p Astrand. Quantification of exercise capability and evaluation of physical capacity in man. *Progress in Cardiovascular Diseases*, 19:154–163, 1976.
- [3] P Baldissera. Proposal of a coast-down model including speed-dependent coefficients for the retarding forces. *Journal of Sports Engineering and Technology*, 231:154–163, 2017.
- [4] N Barry, T Burton, J Sheridan, M Thomson, and A T Brown. Aerodynamic drag interactions between cyclists in a team pursuit. *Sports Engineering*, 18:93–103, 2015.
- [5] J C Bartram, D Thewlis, D T Martin, and K I Norton. Accuracy of w' recovery kinetics in high performance cyclists - modelling intermittent work capacity. *International Journal of Sports Physiology and Performance*, 0:0, 2016.
- [6] J C Bartram, D Thewlis, D T Martin, and K I Norton. Predicting critical power in elite cyclists: Questioning validity of the 3-min all-out test. *Journal of Sport Physiology and Performance*, IN PRESS.
- [7] H C Bergstrom, J M Housh T J and, Zuniga, D A Traylor, R W Lewis, C L Camic, R J Schmit, and G O Johnson. Differences among estimates of critical power and anaerobic work capacity derived from five mathematical models and the three minute all-out test. *Journal of Strength and Conditioning Research*, 28:592–600, 2014.
- [8] B Blocken, T Defraye, E Konincks, J Carmeliet, and P Hespel. Cfd simulations of the aerodynamic drag of two drafting cyclists. *Computers & Fluids*, 71:435–445, 2013.
- [9] B Blocken, T Defraye, E Konincks, J Carmeliet, and P Hespel. Surprises in cycling aerodynamics. *Euro Physics News*, 44:20–23, 2013.
- [10] J P Broker, C R Kyle, and Burke E R. Racing cyclist power requirements in the 4000-m individual and team pursuits. *Medicine and Science in Sports and Exercise*, 31:1677–1685, 1999.
- [11] R Candau, F Grappe, M Ménard, B Barbier, G Y Millet, M D Hoffman, A R Belli, and J D Roullion. Simplified deceleration method for assessment of resistive forces in cycling. *Medicine and Science in Sports and Exercise*, 31:1441–1447, 1999.
- [12] R Candau, F Grappe, M Ménard, B Barbier, G Y Millet, M D Hoffman, A R Belli, and J D Roullion. Simplified deceleration method for assessment of resistive forces in cycling. *Medicine and Science in Sports and Exercise*, 31:1441–1447, 1999.
- [13] A J Chipperfield, P Fleming, and H Pohlheim. A genetic algorithm toolbox for matlab. In *Proc. Tenth International Conference on Systems Engineering (ICSE, Coventry, UK, September 1994)*, pages 200–207, Coventry, UK, 1994. Research Gate.
- [14] Jos J De Koning, Maarten F Bobbert, and Carl Foster. Determination of optimal pacing strategy in track cycling with an energy flow model. *Journal of Medicine in Sport*, 2:266–277, 1999.
- [15] P Debraux, F Grappe, A V Manolova, and W Bertucci. Aerodynamic drag in cycling: methods of assessment. *Sports Biomechanics*, 10:197–218, 2011.
- [16] T Defraye, B Blocken, E Konincks, P Hespel, P Verboven, B Nicolai, and J Carmeliet. Cyclist drag in team pursuit: Influence of cyclist sequence stature, and arm spacing. *Journal of Biomechanical Engineering*, 136:011005–1–011005–9, 2014.

- [17] W. C. Edwards, A. G. & Byrnes. Aerodynamic characteristics as determinants of the drafting effect in cycling. *Med. Sci. Sports Exerc.*, 39:170–176, 2007.
- [18] B Fitton, O Caddy, and D Symons. The impact of relative athlete characteristics on the drag reductions caused by drafting when cycling in a velodrome. *Journal of Sports Engineering and Technology*, 232:39–49, 2018.
- [19] C Foster, J J De Koning, F Hettinga, J Lampen, K L La Clair, C Dodge, M Bobbert, and J P Porcari. Pattern of energy expenditure during simulated competition. *Medicine and Science in Sports and Exercise*, 35: 826–831, 2003.
- [20] R. L. Haupt. Optimum population size and mutation rate for a simple real genetic algorithm that optimizes array factors. In *IEEE Antennas and Propagation Society International Symposium. Transmitting Waves of Progress to the Next Millennium. 2000 Digest. Held in conjunction with: USNC/URSI National Radio Science Meeting (C, volume 2, pages 1034–1037 vol.2, July 2000. doi: 10.1109/APS.2000.875398.*
- [21] D P Heil. Body mass scaling of frontal area in competitive cyclists not using aero-handlebars. *European Journal of Physiology*, 87:520–528, 2002.
- [22] L Heimans, W R Dijkshoorn, M J M Hoozemans, and J J De Koning. Optimizing the team for required power during track cycling team pursuit. *International Journal of Sports Physiology and Performance*, 12:1385–1391, 2017.
- [23] W Hennekam and J Bontsema. Determination of f_r and k_d from the solution of the equation of motion of a cyclist. *European Journal of Physics*, 12:59–63, 1999.
- [24] F J Hettinga, J J de Koning, and Foster C. Relative importance of pacing strategy and mean power output in 1500-m self-paced cycling. *British Journal of Sports Medicine*, 46:30–35, 2012.
- [25] D J Housh, T J Housh, and S M Bauge. A methodological consideration for the determination of critical power and anaerobic work capacity. *Exercise and Sport*, 61(4):406–409, 1990.
- [26] ICU. Icu cycling regulations - part 2 road races. online <http://www.uci.ch/inside-uci/rules-and-regulations/regulations/>, October 2017.
- [27] A Íñiguez de-la Torre and J Íñiguez. Aerodynamics of a cycling team in a time trial: does the cyclist at the front benefit? *European Journal of Physics*, 30:1365, 2009.
- [28] D Jenkins, K Kretek, and D Bishop. The duration of predicting trial influences time to fatigue at critical power. *Journal of Science and Medicine in Sports*, 1(4):213–218, 1998.
- [29] C R Kyle. Reduction of wind resistance and power output of racing cyclists and runners traveling in groups. *Ergonomics*, 22:387–397, 1979.
- [30] H. Monod and J. Scherrer. The work capacity of a synergic muscular group. *Ergonomics*, 8:329–338, 1965.
- [31] H R Morton. Modeling human power endurance. *Journal of Mathematical Biology*, 28:49–64, 1990.
- [32] H R Morton. The critical power and related whole-body bioenergetic models. *European Journal of Applied Physiology*, 96:339–354, 2006.
- [33] R H Morton. A three component model of human bioenergetics. *Journal of Mathematical Biology*, 24: 451–466, 2004.
- [34] R H Morton and L V Billat. The critical power model for intermittent exercise. *European Journal of Applied Physiology*, 91:303–307, 2004.
- [35] D A Noordhof, Skiba P E, and J J de Koning. Determining anaerobic capacity in sporting activities. *International Journal of Sports Physiology and Performance*, 8:475–482, 2013.
- [36] T S Olds, K I Norton, and N P Craig. Mathematical model of cycling performance. *Journal of Applied Physiology*, 75:730–737, 1993.

- [37] T S Olds, K I Norton, E L A Lowe, F Olive, and S Ly. Modeling road cycling performance. *Journal of Applied Physiology*, 78:1596–1611, 1995.
- [38] S Padilla, I Mujika, F Angulo, and Goiriena J J. Scientific approach to the 1-h cycling world record: a case study. *Journal of Applied Physiology*, 89:1522–1527, 2000.
- [39] P. E. Prampero, di. Cycling on earth, in space, on the moon. *European Journal of Applied Physiology*, 82:345–360, 2000.
- [40] P. E. Prampero, di, Gortili G., P. Mognoni, and F. Saibene. Equations of motion of a cyclist. *Journal of Applied Physiology*, 47:201–206, 1979.
- [41] Margaria R. *Biomechanics and energetics of muscular exercise*. Oxford university press, 1976.
- [42] Gordon S. Optimising distribution of power during a cycling time trial. *Sports Engineering*, 8:81–90, 2005.
- [43] F. P. Skiba, W Chidnok, A Vanhatalo, and A. M. Jones. Modeling the expenditure and reconstruction of work capacity above critical power. *American college of sports medicine*, 44:1526–1532, 2012.
- [44] VS Sreedhara, G M Mocko, and R E Hutchison. An experimental protocol to model recovery of anaerobic work. *Proceedings*, 2:208, 2018.
- [45] L Underwood and M Jeremy. Mathematical model of track ccling: the individual pursuit. *Procidia engineering*, 2:3217–3222, 2010.
- [46] G. J. Van Ingen Schenau and P. R. Cavanagh. Power equations in endurance sports. *Journal of Biomedics*, 23:865–881, 1990.
- [47] H Vandewalle. Critical power test for ramp exercise. *Journal of Applied Physiology*, 71:285–286, 1995.
- [48] A Vanhatalo, J H Doust, and Burnley M. Determination of critical power using a 3-min all-out cycling test. *Medicien in Sports and Exercise*, 39(3):548–555, 2007.